The function of Prdm12 in histone methylation and cell proliferation

Yang Chia-Ming

Abstract

This study investigated the function of Prdm12 by examining its histone methyltransferase activity by an *in vitro* methylation assay. The result showed that expressed Prdm12 isolated from the mammalian cell line methylated histone H3K9. However, some members of the Prdm family have extrinsic enzymatic activities and interact with known histone methyltransferases such as G9a, a strong H3K9 methyltransferase. Therefore, this possibility was explored, and Prdm12 was found to also interact with G9a. The domain required for G9a binding was also examined, and plasmids expressing deletion or point mutants of Prdm12 were constructed. Co-immunoprecipitation assay results indicated that the second zinc finger (ZF) domain was required for G9a interaction. As expected, the histone methyltransferase activity of Prdm12 depended on the interaction with G9a because the Prdm12 mutants defective in G9a binding did not methylate histone H3. Next, the biological function of Prdm12 was investigated, and the importance of histone methyltransferase activity in Prdm12 function was determined. Because Prdm12 is expressed in the developing mouse central nervous system, P19 embryonic carcinoma cells, an *in vitro* model for neural differentiation, were used to investigate the function of Prdm12. Results showed that during retinoic acid (RA)-induced neural differentiation in P19 cells, both mRNA and protein expression of

Prdm12 increased. To elucidate the role of Prdm12 in this process, short hairpin RNA (shRNA) was used to stably knock down Prdm12 in P19 cell lines. These cell lines were subjected to RA-induced neural differentiation. At the first aggregation stage, the cell number of Prdm12 knockdown cells was more than that of control cells. After differentiation, the cells were immunostained with a mature neuronal marker, class III β-tubulin (Tuj1). The percentage of Tuj1-positive cells was almost the same between Prdm12 knockdown and control cells. To further evaluate the function of Prdm12 in cell proliferation, Prdm12 and mutants were overexpressed in P19 cells. Cells were counted every 2 days, and the growth curve was calculated. The result indicated that Prdm12 decreased the proliferation of P19 cells, and both the PR (PRDI-BF1-RIZ1 homologous) and ZF domains were required for its antiproliferative function. However, overexpressing Prdm12 in NIH3T3 cells did not affect cell growth. This result suggested that Prdm12 may be involved in a pathway specific to stem cells. Next, the mechanism of the antiproliferative effect of Prdm12 was investigated. Because cell death was not observed in Prdm12-overexpressing P19 cells, Prdm12 may regulate the cell cycle. Flow cytometric analysis showed that Prdm12 increased the G1 population. Further, western blot analysis showed that the expression of the cyclin-dependent kinase inhibitor p27 increased in Prdm12-overexpressing P19 cells. This result was consistent with

a previous report showing that RA increased the number of G1-phase cells and the expression of p27 in P19 cells. The results of the present study showed that RA induced Prdm12 in P19 cells, and Prdm12 exerted antiproliferative effects in part through regulation of the G1 phase of the cell cycle. Furthermore, ectopic Prdm12 increased the expression of p27, with both the PR and ZF domains being necessary for its function.

Table of Contents

page

Abbreviations

PR domain	PRDI-BF1-RIZ1 homologous domain
ZF domains	kruppel type zinc finger domains
HKMTase	histone lysine methyltransferases
RA	retinoic acid

Chapter 1: Introduction

1-1. Histone lysine methyltransferases

Different lysine (K) sites of various histones are mono-, di-, or tri-methylated by the SET [SU(VAR)3-9, E(Z), trithorax] domain protein methyltransferase superfamily. The SET domain is the catalytic domain conserved in this superfamily. Depending on the modification of different lysine sites, it could transcriptionally activate or repress gene expression. For example, methylation of K26 in histone H1; K9, K27, and K36 in histone H3; and K20 in histone H4 is associated with transcriptional silencing. In contrast, methylation of K4 in histone 3 is associated with transcriptional activation (Fig. 1-1; see Dillon *et al.*, 2005 for a review).

1-2. Structural features and biological function of the Prdm family

The Prdm family contains a PR (PRDI-BF1-RIZ1 homologous) domain in the N terminus, which has a 20–30% sequence identity to the conserved catalytic SET domains of the histone lysine methyltransferase (HKMTase) superfamily (Fig. 1-2; Völkel *et al.*, 2007). This similarity suggests that the Prdm family may have HKMTase properties. In fact, some Prdms show

intrinsic HKMTase activity (Prdm2, Prdm3, Prdm8, Prdm9, and Prdm16). In addition, Prdm1, Prdm5, and Prdm6 lack intrinsic HKMTase activity, but instead recruit G9a/Ehmt2/KMT1C, a strong mammalian histone H3 lysine 9 (H3K9) methyltransferase, to mediate HKMTase activity (see Fog *et al.*, 2012 for a review). Another structural feature of the Prdm family is the presence of multiple Krüppel-type zinc finger (ZF) domains in the C terminus involved in sequence-specific DNA binding and protein-protein interactions (Völkel *et al.*, 2007).

It has been reported that the Prdm family is expressed dynamically in the nervous system during the development of mice and zebrafish (Hohenauer *et al.*, 2012). The function of the Prdms in neurogenesis remains unclear, however. In zebrafish embryos, Prdm1 is important for the development of neural crest and sensory neurons (Hernandez-Lagunas *et al.*, 2005). Our laboratory has previously described the expression pattern of Prdm8 in the mouse embryonic nervous system (Komai *et al.*, 2009). Another study using a knockout mouse model indicated that Prdm8 is involved in neural development (Ross *et al.*, 2012).

1-3. Expression of Prdm12 in the nervous system

Prdm12 expression was observed in the spinal cord, caudal forebrain, and midbrain of mouse E9.5 embryos by whole-mount *in situ* hybridization (Kinameri *et al.*, 2008). In zebrafish, Prdm12 was expressed in the olfactory placode, tegmentum, cerebellum, and hindbrain at 48 hours post-fertilization (Sun *et al.*, 2008). Although Prdm12 has been reported to be expressed in the mouse and zebrafish embryonic nervous system (Kinameri *et al.*, 2008; Sun *et al.*, 2008), the role of Prdm12 is still unclear.

1-4. Retinoic acid-induced neural differentiation in P19 embryonic carcinoma cells

Retinoic acid (RA) is a metabolite of vitamin A (retinol), which controls neural differentiation and patterning (Maden, 2007). To investigate the process of neural differentiation *in vitro*, P19 embryonic carcinoma cells were used as a model system. Treatment with RA under aggregating conditions induced P19 embryonic carcinoma cells to differentiate into neurons and glia (Jones-Villeneuve *et al.*, 1982). Upregulation of p27, a cyclin-dependent kinase inhibitor (CKI), has been shown to be involved in

arresting cell cycle progression at the G_1 phase in this *in vitro* model (Gill *et al.*, 1998). Furthermore, overexpression of p27 could induce neural differentiation in mouse neuroblastoma cells (Kranenburg *et al.*, 1995).

1-5. Research purpose

Since many Prdms have HKMTase properties, it is of interest whether Prdm12 also has HKMTase properties. This study first demonstrates that Prdm12 recruits G9a to methylate H3K9. Because the localization of Prdm12 in the embryonic nervous system implies a potential function in neurogenesis, this study investigates the role of Prdm12 in the RA-induced neural differentiation of P19 cells as a model system.

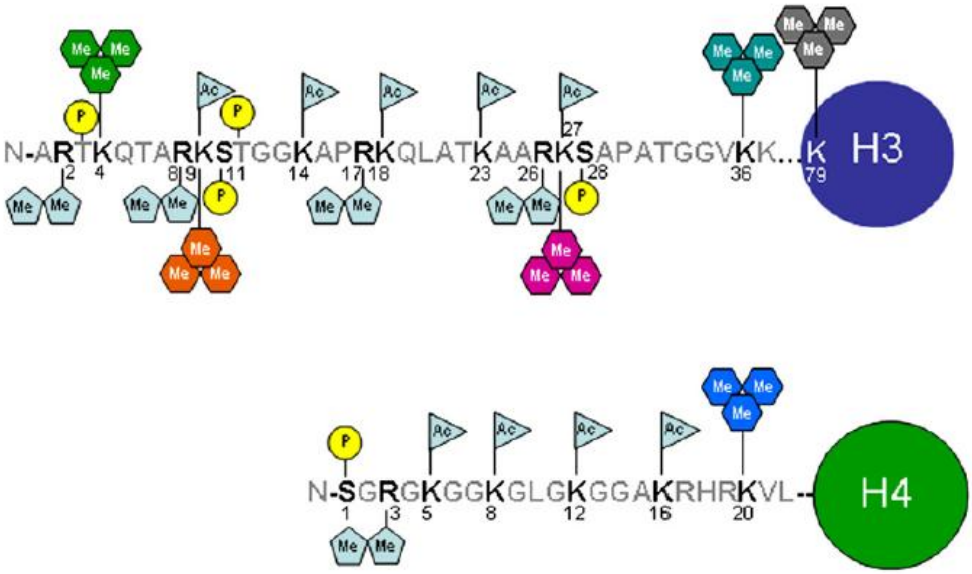

Fig. 1-1: Schematic diagram of Histone modifications. The modifications include methylation (Me), acetylation (Ac), phosphorylation (P) and ubiquitination (Ub). This picture is cited from Völkel *et al.*, 2007.

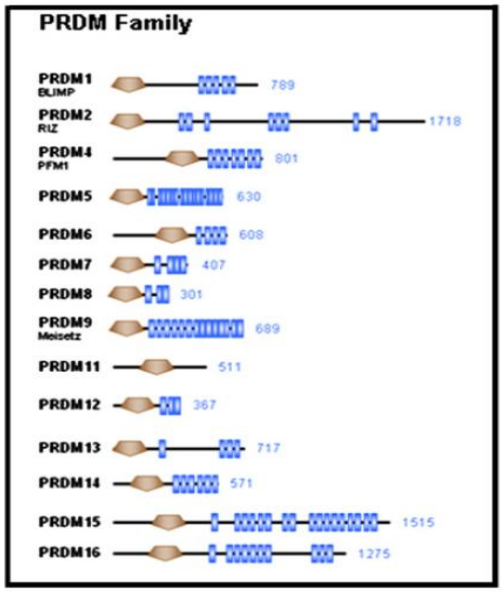

Fig. 1-2: Structural features of Prdm family. The Prdm gene family contains 16 members in mice. Prdm family has a PR domain in the N-terminal and several zinc finger domains in the C-terminal except Prdm11. Prdm12 has three ZF domains. This picture is cited from Völkel *et al.*, 2007.

Chapter 2: Results

Section 1: The Prdm12 complex exhibits H3K9 methyltransferase activity through interaction of G9a with ZF domains

2-1-1 Prdm12 methylates histone H3 as revealed by an *in vitro* methylation assay

Prdm12 was hypothesized to have HKMTase properties. To investigate the potential HKMTase properties of Prdm12, enhanced green fluorescent protein (EGFP)-tagged Prdm12 (EGFP-Prdm12), EGFP-tagged Prdm4, and EGFP were expressed in and purified from HEK293T cells for *in vitro* methylation assays, using core histones as substrates. The glutathione *S*-transferase (GST)-fused catalytic SET domain of G9a (GST-G9aSET) was added as a positive control. EGFP-Prdm12 showed higher H3 methylation than EGFP or EGFP-Prdm4 (Fig. 2-1), suggesting that EGFP-Prdm12 can methylate histone H3.

2-1-2 Prdm12 methylates the K9 site of histone H3

Next, the H3 site methylated by Prdm12 was determined. To this end,

GST-fused histone H3 amino-terminus (residues 1–57, GST-H3N) and mutants in which single K substitutions were introduced to lysine 4, 9, or 27 (GST-H3NK4R, GST-H3NK9R, and GST-H3NK27R) were purified from *Escherichia coli* as substrates for the *in vitro* methylation assay (Fig. 2-2A). GST-H3N, GST-H3NK4R, and GST-H3NK27R, but not GST-H3NK9R, were methylated by EGFP-Prdm12 (Fig. 2-2B). To further examine the methylation type of H3K9, anti-H3K9me1, anti-H3K9me2 and anti-H3K9me3 antibody were used for western blot analysis. Recombinant H3 incubated with EGFP-Prdm12 was di-methylated on H3K9 (Fig. 2-2C). These results indicate that EGFP-Prdm12 specifically di-methylates lysine 9 of histone 3 (H3K9).

2-1-3 Prdm12 alone cannot methylate histone H3

Whether the HKMTase activity of Prdm12 was intrinsic or extrinsic was further investigated; GST-fused Prdm12 (GST-Prdm12) was expressed in and purified from *E. coli* and examined by an *in vitro* methylation assay. HKMTase activity was not observed in GST-Prdm12 (Fig. 2-3). These results imply that Prdm12 may lack intrinsic HKMTase activity, but instead forms

complexes with other enzymes that have H3K9 methyltransferase properties.

2-1-4 Prdm12 binds with G9a but not with GLP or ESET

Prdm1, Prdm5, and Prdm6 were reported to mediate HKMTase activity by recruiting G9a. To examine whether Prdm12 interacts with G9a in a similar manner, co-immunoprecipitation (Co-IP) assays were performed. EGFP-Prdm12 and FLAG-tagged G9a (FLAG-G9a) were transiently expressed in HEK293T cells. The IP complex was isolated with either anti-FLAG or anti-EGFP antibody from cell extracts. Immunoprecipitation of EGFP-Prdm12 co-isolated the FLAG-G9a complex and vice versa (Fig. 2-4A). Next, whether Prdm12 could bind to other H3K9 HKMTases (here GLP/Ehmt1/KMT1D and ESET/Setdb1/KMT1E were used) was examined, but no interactions between EGFP-Prdm12 and FLAG-GLP or FLAG-ESET were detected by Co-IP analysis (Fig. 2-4B). These results indicate that Prdm12 specifically forms a complex with G9a. The interaction between Prdm12 and G9a in intact cells was further confirmed by immunocytochemistry by transiently expressing EGFP-Prdm12 and

FLAG-G9a in HEK293T cells. EGFP-Prdm12 and FLAG-G9a colocalized primarily to the nuclear periphery (Fig. 2-4C). These results suggest that Prdm12 and G9a form a complex in intact cells.

2-1-5 Interaction with G9a through ZF domains is necessary for the HKMTase activity of Prdm12

The study next determined which Prdm12 domain interacts with G9a, using FLAG-Prdm12 to make PR or ZF domain deletion mutants (FLAG-Prdm12ΔPR, FLAG-Prdm12ΔZF) and a series of point mutants (Fig. 2-5A). In the point mutants, G115 or F117 (two conserved sites in PR domain) was replaced with alanine (FLAG-Prdm12G115A, FLAG-Prdm12F117A), and the structure of the first or second ZF domains was disrupted by replacing the two cysteines in C2H2 with arginine (FLAG-Prdm12Z1-, FLAG-Prdm12Z2-). These mutants and G9a were used in the Co-IP assays. Except for FLAG-Prdm12ΔZF and FLAG-Prdm12Z2-, FLAG-Prdm12 and the other mutants bound to G9a (Fig. 2-5B, C). These results showed that the second ZF domain was necessary for Prdm12 to associate with G9a.

It was then determined whether the HKMTase activity of Prdm12 was correlated with its association with G9a. To this end, FLAG-Prdm12 and mutants were isolated from HEK293T cells for an *in vitro* methylation assay. The FLAG-Prdm12ΔZF and FLAG-Prdm12Z2- complexes lacking G9a binding capacity did not methylate histone H3 (Fig. 2-5D). This result suggests that the HKMTase activity of Prdm12 depends on the association between Prdm12's second ZF domain and G9a.

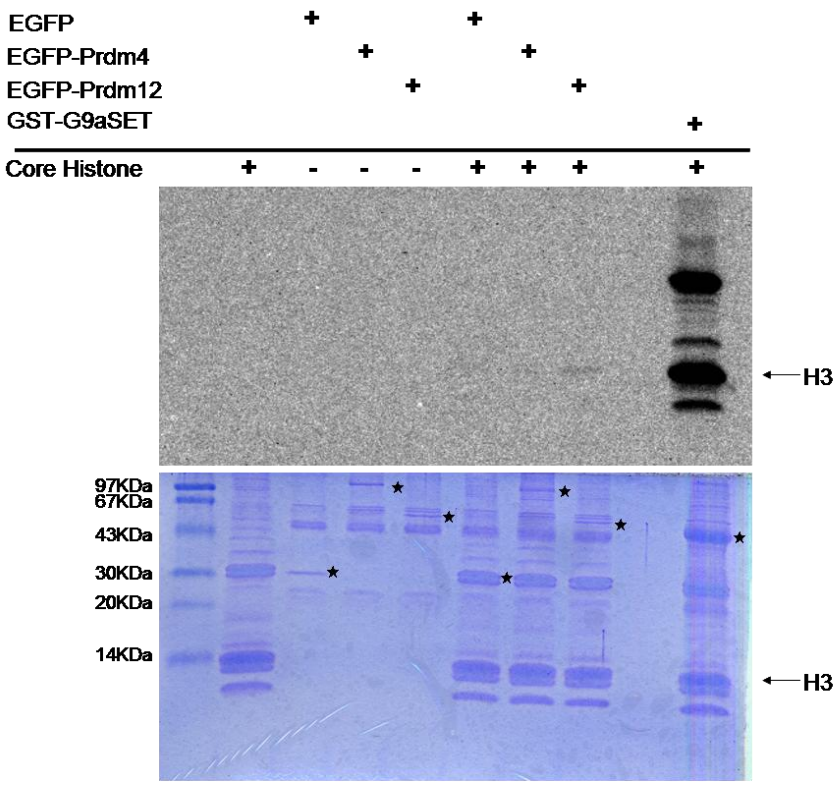

Fig. 2-1: In vitro methylation assay. EGFP-Prdm12, EGFP-Prdm4, or GFP plasmids were transiently transfected into HEK293T cells and expressed products were purified by anti-GFP antibodies. GST-G9aSET produced in *E. coli* and purified with glutathione-Sepharose beads was used as a positive control. The immunoprecipitated complex was incubated with 2 μg of core histones as substrates and S-adenosyl-[methyl-C14]-L-methionine as a methyl donor. After incubation for 60 min at 30°C, samples were subjected to 15% SDS-PAGE. Methylated histones were detected by autoradiography (top). The amount of protein was shown by coomassie brilliant blue (bottom). ★, EGFP, EGFP- or GST-fusion molecules.

A

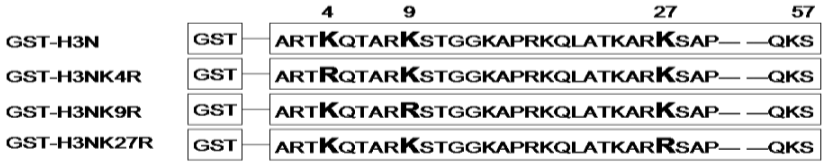

B

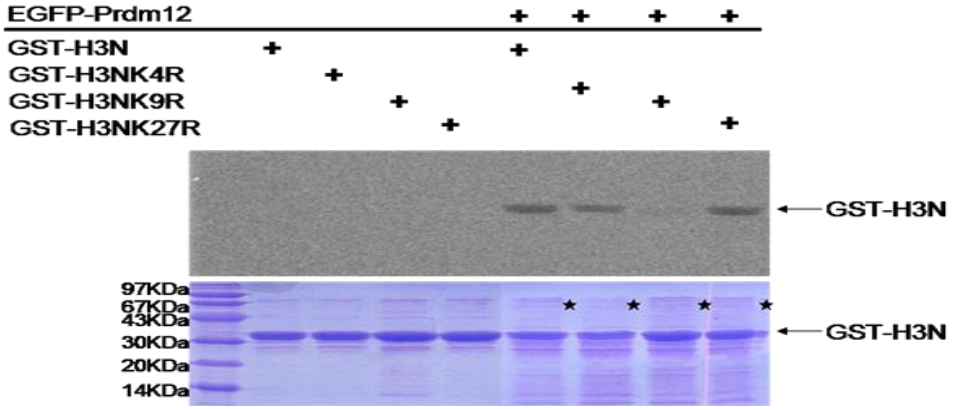

C

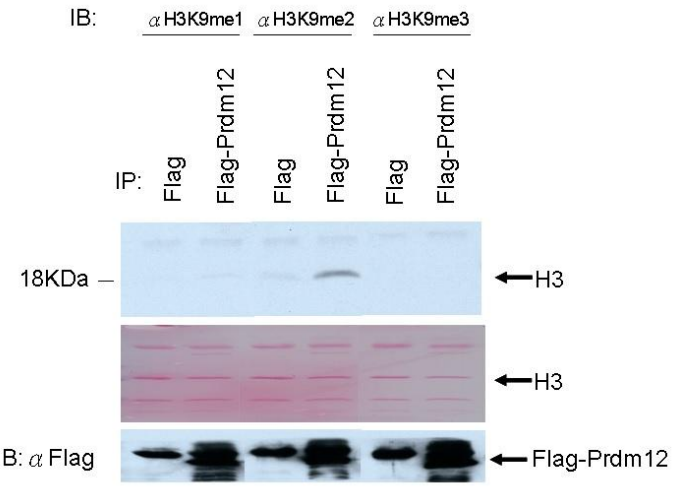

Fig. 2-2: (A) Schematic diagram of GST-H3N and point mutants (Tachibana *et al.* 2001). Residues 1–57 of the N-terminal of histone H3 were fused to GST. The lysine (K) was replaced by arginine (R) at the indicated position. (B) Two micrograms of GST-H3N or mutants were used as substrates for

the *in vitro* methylation assay as described in Fig. 2-1. ★, EGFP-Prdm12.

(C) Two micrograms of recombinant H3/H4 were used as substrates for *in vitro* methylation assay as described in Fig. 2-1 except non-isotope-labeled SAM were used. Different types of H3K9 methylation were detected by specific antibody.

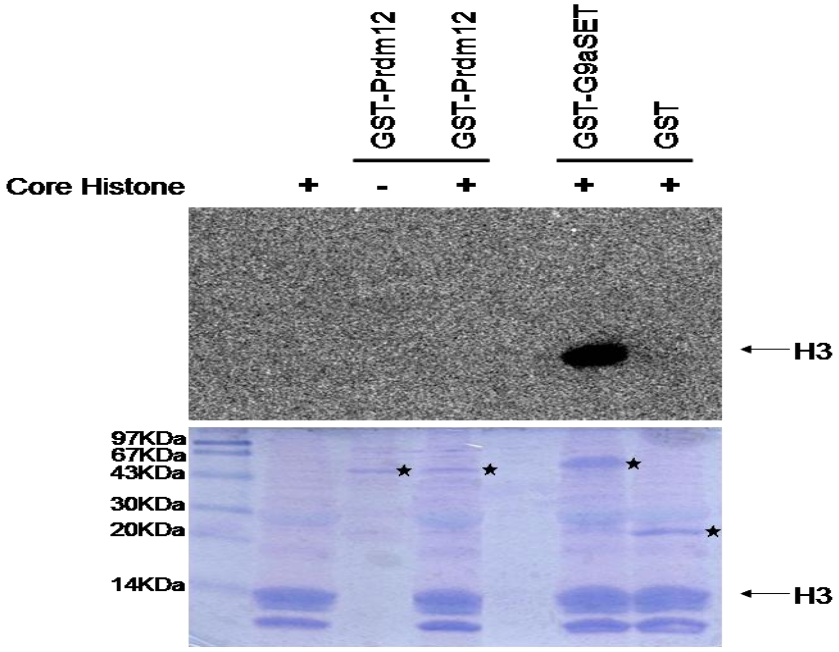

Fig. 2-3: GST-Prdm12, GST-G9aSET, and GST were expressed in E. coli and purified with glutathione-Sepharose beads. One microgram of each enzyme was incubated with 2 μg of core histones as substrates for in vitro methylation assay. Methylated histones were detected by autoradiography (top). The amount of protein was revealed by coomassie brilliant blue (bottom). ★, GST or GST-fusion molecules.

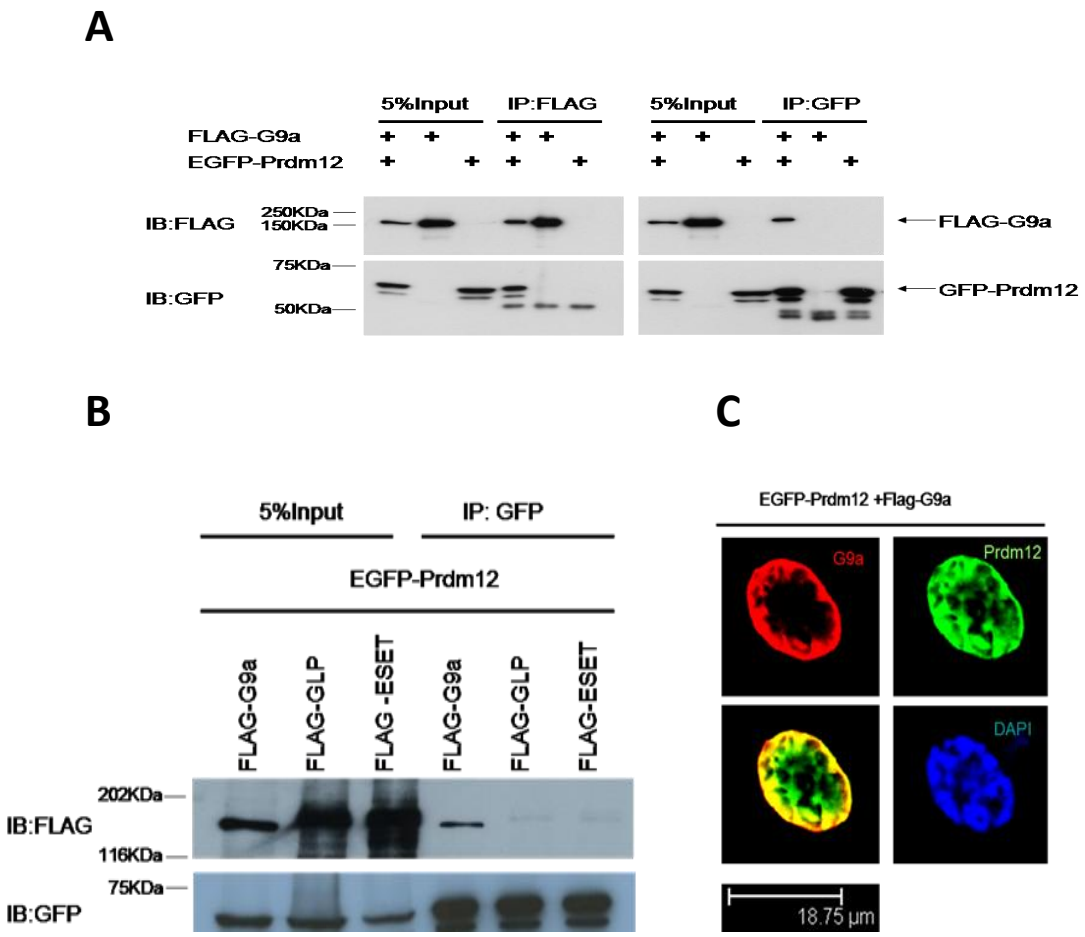

Fig. 2-4: The second ZF domain of Prdm12 is required for G9a association and HKMTase activity. (A) Co-immunoprecipitation (Co-IP) of G9a and Prdm12. HEK293T cells were co-transfected with plasmids encoding EGFP-Prdm12, FLAG-G9a or both. Top, anti-FLAG blots for G9a. Bottom, anti-GFP blots for EGFP-Prdm12. (B) Co-IP of EGFP-Prdm12 with H3K9 methyltransferase indicated above the panel (FLAG-G9a, FLAG-GLP, or FLAG-ESET). Cell lysates from HEK293T cells transfected with a combination of plasmids were subjected to IP using an anti-GFP antibody. Immunoprecipitates were then subjected to western blot analysis with

anti-FLAG (top) or anti-GFP (bottom) antibody. (C) NIH-3T3 cells were co-transfected with plasmids expressing EGFP-Prdm12 and FLAG-G9a. After fixation, cells were double-immunostained for GFP-Prdm12 (green) and FLAG-G9a (red). Co-localization was observed by confocal immunofluorescence microscopy.

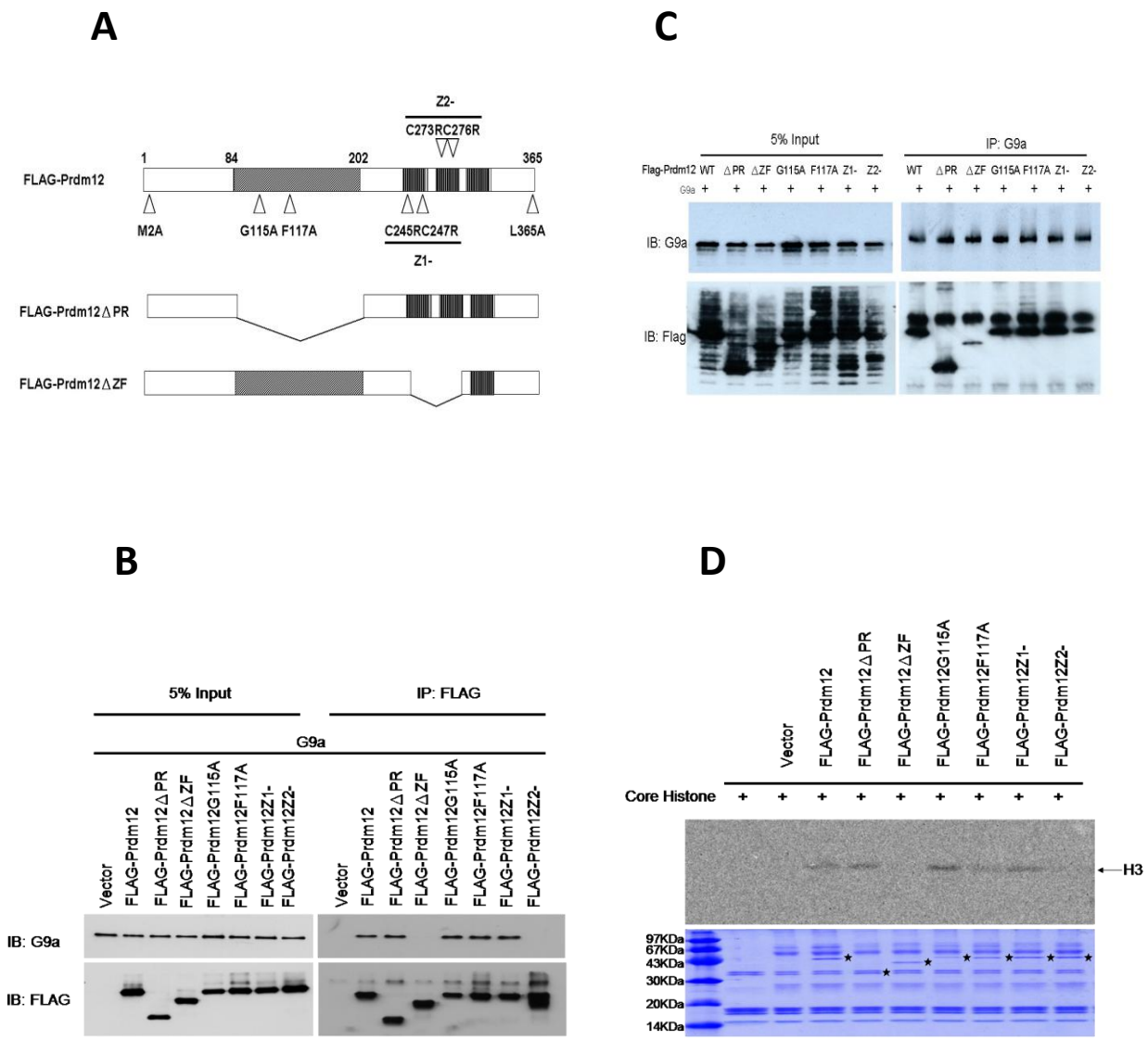

Fig. 2-5: (A) Schematic diagram of FLAG-Prdm12 and mutants. Numbers indicate the amino acids that were replaced. Point mutation (Δ), deletion (⋁). (B-C) Co-IP determined that the ZF domains of Prdm12 interacted with G9a. HEK293T cells were co-transfected with plasmids encoding G9a and FLAG-Prdm12 or the mutants described in (A). Lysates were immunoprecipitated with anti-FLAG antibody (B) or anti-G9a antibody (C). Immunoprecipitates were then subjected to western blot analysis with

anti-G9a (top) or anti-FLAG (bottom) antibody. (D) FLAG-Prdm12 WT or mutants were transfected into HEK293T cells, then immunoprecipitated with anti-FLAG antibody. Immunoprecipitates were subjected to the *in vitro* methylation assay. Methylated Histone H3 (top). The amounts of proteins were revealed by coomassie brilliant blue (bottom). ★, FLAG-Prdm12 WT and mutants.

Section 2: Generation of rabbit anti-Prdm12 polyclonal antibody

2-2-1 Purification of rabbit anti-Prdm12 polyclonal antibodies

To detect Prdm12 proteins expression, rabbit anti-Prdm12 polyclonal antibody was generated. The process is illustrated in Fig. 2-6A and the details are mentioned in the Materials and Methods. Briefly, GST-Prdm12 (43-230) proteins were expressed in *Escherichia coli* (Fig. 2-6B) then purified by glutathione-Sepharose beads (Fig. 2-6C) and cross-linked to the beads (Fig. 2-6D). Next, serum from rabbit immunized with GST-Prdm12 (43-230) was incubated with GST cross-linked beads first to remove anti-GST polyclonal antibody. Then the serum was incubated with GST-Prdm12 (43-230) cross-linked beads. After wash with TBS, bound antibodies were eluted. 10 fractions were collected and the fractions contained antibodies were identified by coomassie brilliant blue staining. Fraction 2 and 3 were combined and dialyzed in PBS buffer (Fig. 2-6E).

2-2-2 Sensitivity and specificity of rabbit anti-Prdm12 polyclonal antibodies

To check the activity of purified rabbit anti-Prdm12 polyclonal antibodies, anti-Prdm12 polyclonal antibodies were used to detect

EGFP-Prdm12 protein by western blot analysis. Fig. 2-7A shows that 4,000-fold diluted anti-Prdm12 still could detect clear band. The purified rabbit anti-Prdm12 also could immunoprecipitated Prdm12 (Fig. 2-7B). Finally, the specificity of rabbit anti-Prdm12 polyclonal antibodies was examined. The purified anti-Prdm12 only recognized EGFP-Prdm12 but not EGFP-Prdm4, EGFP-Prdm6 and EGFP-Prdm13 (Fig. 2-7C). These results indicated application of purified rabbit anti-Prdm12 polyclonal antibodies for western blot and immunoprecipitation assays.

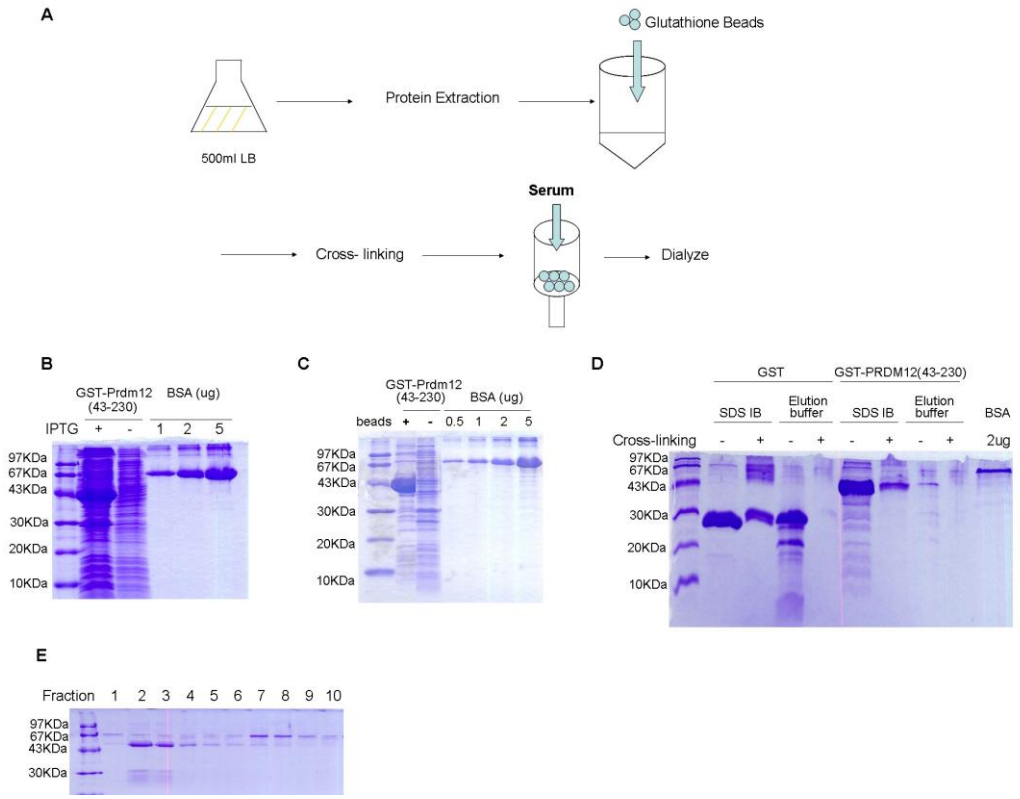

Fig. 2-6: (A) Schematic diagram of purification of anti-Prdm12 antibodies. Details are described in the Materials and Methods. (B) Induction of GST-Prdm12 (43-230) by IPTG in *Escherichia coli*. Bovine serum albumin (BSA) was used to compare the protein amount of GST-Prdm12 (43-230). (C) GST-Prdm12 (43-230) protein was purified by 2 ml of 50% slurry of glutathione sepharose beads. (D) GST or GST-Prdm12 (43-230) proteins were cross-linked to glutathione sepharose beads by dimethyl pimelimidate. After cross-link, no binding proteins were eluted. SDS sample buffer were used to evaluate the cross-linking efficiencies. (E) Eluted fractions were collected. 5μl of each fraction was separated by 12%-PAGE. All the gels were visualized by coomassie brilliant blue staining.

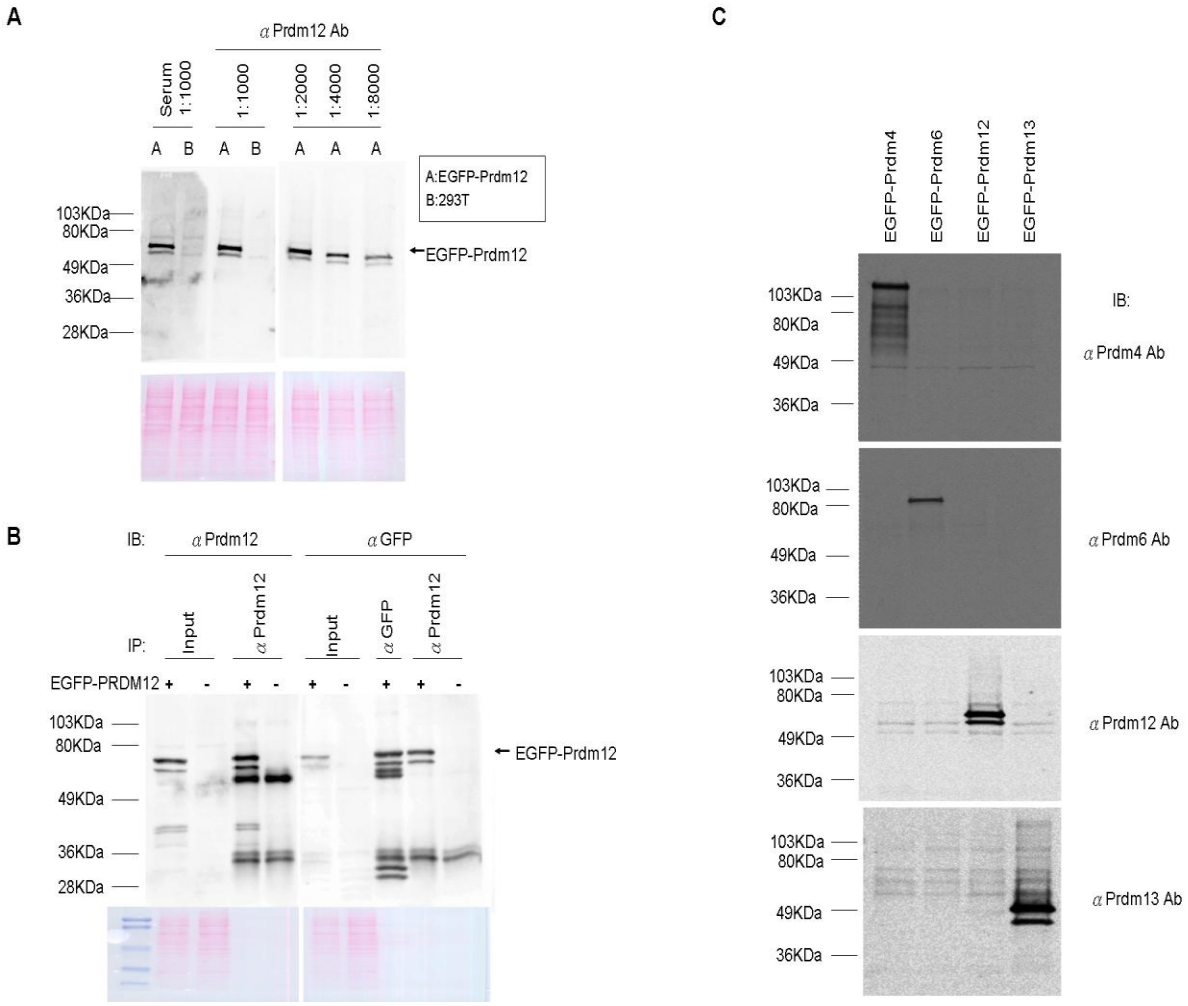

Fig. 2-7: (A) Anti-Prdm12 antibodies were serial diluted to detect EGFP-Prdm12 by western blot analysis. A: cell lysates contained over-expressed EGFP-Prdm12. B: HEK293T cell lysates were used as negative control. Original serum was used as a positive control. (B) Anti-Prdm12 antibodies could be used for immunoprecipitation. Anti-GFP antibody was used as a positive control. The EGFP-Prdm12 proteins isolated by anti-Prdm12 antibody were also confirmed by anti-GFP antibodies. (C) EGFP-Prdm4, EGFP-Prdm6, EGFP-Prdm12 or EGFP-Prdm13

was transfected into HEK293T cells. Cell lysates were subjected for western blot analysis. Anti-Prdm4, anti-Prdm6, anti-Prdm12 or anti-Prdm13 antibody was used for detection of the corresponding proteins.

Section 3: Retinoic acid induces the expression and antiproliferative activity of Prdm12 in P19 embryonic carcinoma cells

2-3-1 Retinoic acid induces the mRNA and protein expression of Prdm12 in P19 cells

Because Prdm12 is expressed in the nervous system from the early embryogenesis stage (Kinameri *et al*., 2008), and because Prdms have functions in cell differentiation during the developmental processes (Fog *et al*., 2012), the possible role of Prdm12 in neurogenesis was investigated. P19 embryonic carcinoma cells are a well-established *in vitro* model for the study of neural differentiation. In this model, P19 cells were grown as aggregates in bacterial-grade dishes in the presence of 1 μM RA. After 4 days, the cell aggregates were transferred to a cell culture dish, and the medium was changed to RA-free medium. After 1 day, 10% serum medium was replaced with 0.5% serum medium for final differentiation (Fig. 2-8A, top). The mRNA expression of Prdm12 was determined by quantitative reverse transcription-polymerase chain reaction (RT-PCR) during this differentiation process. In response to RA, Prdm12 mRNA expression

increased at day 2, peaked at day 4, and then decreased after the withdrawal of RA (Fig. 2-8A, bottom, triangle). Aggregation of the P19 cells without RA caused a temporary increase in Prdm12 mRNA expression at day 2; however, Prdm12 mRNA expression decreased on day 4 (Fig. 2-8A, bottom, closed circle). This result indicated that RA increased and sustained Prdm12 mRNA expression. To monitor the RA-induced neural differentiation of P19, the mRNA expression of the pluripotent transcription factor Oct3/4 and neuronal class III β-tubulin (Tuj1, neural-specific differentiation marker) was determined using quantitative RT-PCR (Fig. 2-8A, bottom). As expected, the expression of Oct3/4 mRNA decreased, and that of Tuj1 increased. Because Prdm12 interacted with G9a, the mRNA and protein expression of G9a was also determined during the differentiation process. Similar to the expression pattern of Prdm12 mRNA, the expression of G9a mRNA increased at days 2 and 4, then decreased at day 5. A point of difference, however, was that G9a mRNA expression increased again at day 7 (Fig. 2-8A, bottom). Whereas the trend of G9a protein expression was similar to that of G9a mRNA expression, GLP protein expression remained stable during differentiation (Fig. 2-8B).

To further confirm the induction of Prdm12 by RA at the protein level, P19 cells were cultured in cell culture dishes or bacterial-grade dishes with or without RA for 4 days. IP-western blot analysis revealed that RA induced Prdm12 protein expression regardless of aggregate formation (Fig. 2-8C, lanes 6 and 8). Concordant with the quantitative RT-PCR results, at day 4 Prdm12 proteins were not detected in the P19 cell suspension in the absence of RA (Fig. 2-8C, lane 7). These results suggest that RA elevates Prdm12 mRNA and protein expression in P19 cells.

2-3-2 Knockdown of Prdm12 in P19 cells increases cell number with RA treatment

Based on the RA-induced expression of Prdm12 in P19 cells, Prdm12 was speculated to play a role in this neuronal differentiation model. To test this hypothesis, two shRNAs (shPrdm12#1 and shPrdm12#2) were made to knockdown Prdm12 expression, and a scrambled shRNA was used as a negative control. After infection and puromycin selection, the knockdown efficiency of stable Prdm12 knockdown P19 cells (P19/shPrdm12) was confirmed by quantitative RT-PCR or IP-western blotting; RA-induced

mRNA and protein expression was efficiently repressed in P19/shPrdm12 cells (Fig. 2-9A and B). These P19/shPrdm12 cells were then used for RA-induced neuronal differentiation. Surprisingly, during the first aggregation stages, RA-treated P19/shPrdm12 cells formed more embryonic bodies than did control cells (Fig. 2-9C). On day 4, the numbers of P19/shPrdm12 cells were directly counted, and were approximately twice the number of the control cells (Fig. 2-9D). After differentiation was induced, the percentage of mature neurons was determined by immunocytochemistry (Tuj1 was used as a marker of mature neurons); no significant difference was found in the percentage of Tuj1-positive neurons between P19/shPrdm12 cells and control P19 cells (Fig. 2-10).

2-3-3 Prdm12 overexpression reduces cell proliferation in P19 cells but not in NIH3T3 cells

The effect of Prdm12 on the growth of P19 cells was further examined. FLAG-Prdm12 constructs and mutants were transfected into P19 cells to produce stable overexpressing cell lines (P19/FLAG-Prdm12, P19/mutants). In addition to the mutants described earlier, two point

mutations were made: the amino acids at the furthest N or C terminus were mutated to be used as controls (FLAG-Prdm12M2A, FLAG-Prdm12L365A; Fig. 2-5A). Cell growth was analyzed by counting the number of cells for 6 days to calculate the cell division times. Compared to P19 cells, the cell division times of the P19/FLAG-Prdm12 cells decreased by approximately 50% at day 6 (Fig. 2-11A). P19/FLAG-Prdm12M2A and P19/FLAG-Prdm12L365A cells still grew as slowly as the P19/FLAG-Prdm12 cells; however, the other P19/mutant cells (with the deletions or point mutations in the PR or ZF domains) lost the ability to inhibit cell proliferation. To determine whether the ability of Prdm12 to impair cell proliferation was cell type specific, NIH3T3 cells were used instead of P19 cells. Cell growth rates were similar between the Prdm12-overexpressing NIH3T3 cells and the control cells (Fig. 2-11B). Taken together, these results suggested that Prdm12 specifically impairs cell proliferation in P19 cells through the PR and ZF domains.

The location of Prdm12 was determined by immunohistochemical analysis of the distribution of Prdm12 and the mutants in the P19 cells. Only FLAG-Prdm12ΔZF moved to the cytoplasm, whereas the other

mutants remained in the nucleus as FLAG-Prdm12 (Fig. 2-12). This finding suggested that some Prdm12 mutants lose their antiproliferative ability, which may not result from mislocalization.

2-3-4 Prdm12 increases the G_1-phase population and p27 expression

Next, the pathway through which Prdm12 regulated the proliferation of P19 cells was investigated. Because cell death was not increased in the P19/Prdm12 cells (data not shown), whether Prdm12 slows cell growth through control of the cell cycle was examined. To this end, the cell cycle distribution of P19 cells expressing FLAG-Prdm12 or deletion mutants was analyzed by flow cytometry. Cell cycle analysis revealed that, compared to the control, the G_1 population of P19/FLAG-Prdm12 cells was increased from 20.6% to 25.7%. FLAG-Prdm12ΔPR and FLAG-Prdm12ΔZF cells showed no changes in cell cycle distribution (Table I). This result suggests that Prdm12 inhibits the proliferation of P19 cells in part through regulation of the G_1 phase of the cell cycle.

The G_1-to-S phase transition is inhibited by cyclin-dependent kinase (CDK) inhibitory proteins (CKIs). The CKIs are classified into two subfamilies:

the INK4 subfamily and the CIP/KIP subfamily. To determine whether Prdm12 increased the G_1 population through upregulation of CKIs, the expression levels of two CKI proteins [p15 (an INK4 member protein) and p27 (a CIP/KIP protein)] were examined in Prdm12- or mutant-overexpressing P19 cells by western blot analysis. The protein expression of p15 did not change, whereas that of p27 increased in P19/FLAG-Prdm12 cells (Fig. 2-13). The results of quantitative RT-PCR showed an upregulation of expression of p27 mRNA in P19/FLAG-Prdm12 cells (data not shown). The expression levels of p15 and p27 remained unchanged in the deletion mutant-overexpressing P19 cells. These data indicated that Prdm12 upregulates p27 expression and that either the PR or ZF domains of Prdm12 are necessary, but not sufficient on their own, for optimal antiproliferative activity of Prdm12.

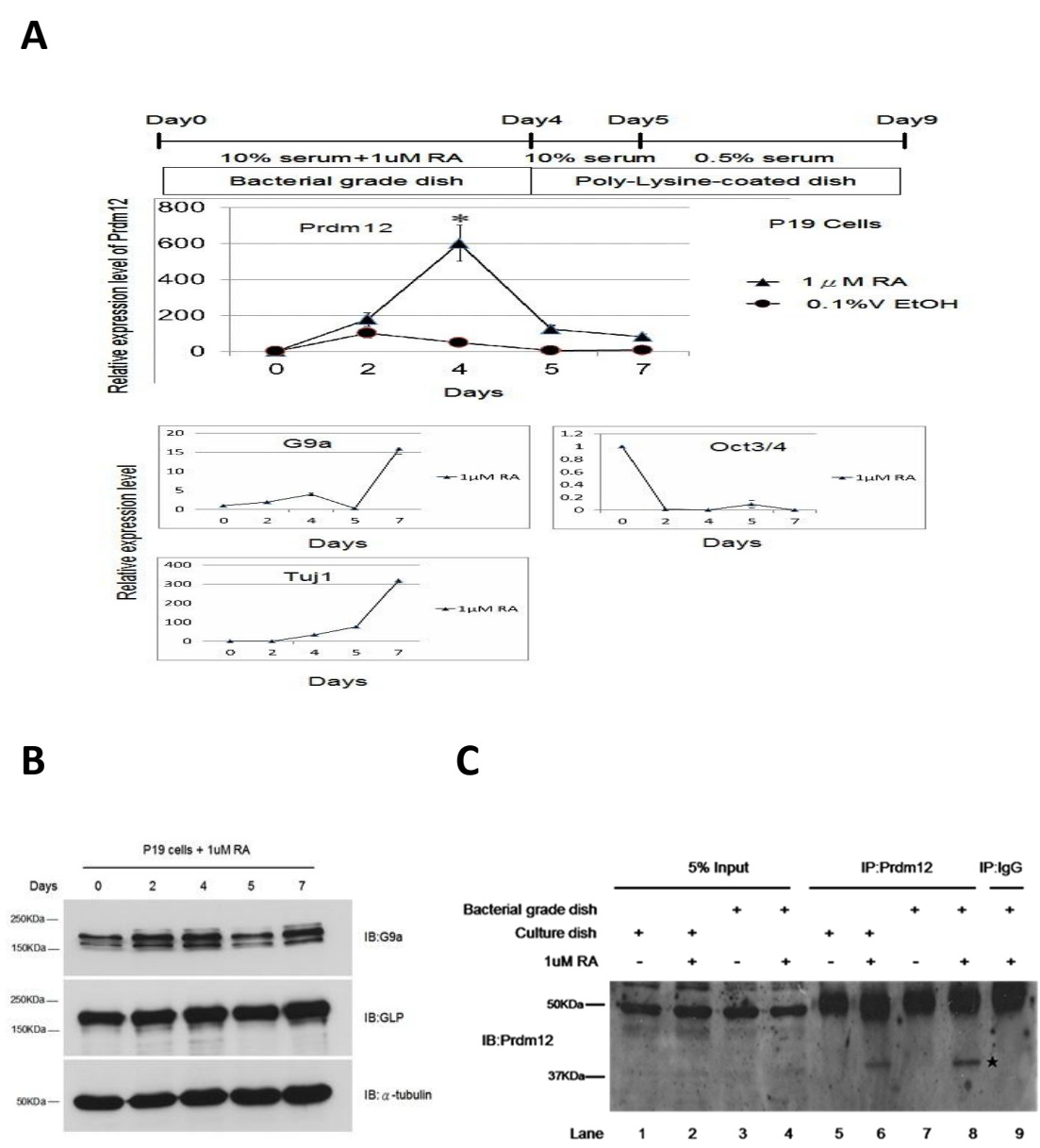

Fig. 2-8: (A) Top, schematic diagram of the protocol for RA-induced neural differentiation in P19 cells. The details are mentioned in the Materials and Methods. Bottom, Prdm12, G9a, Oct3/4 and Tuj1 mRNA levels were determined by quantitative RT-PCR during the differentiation process. 0.1%V EtOH, negative control. Error bars represent the s.d., * $p < 0.05$ versus EtOH control at day 4. (B) The expression of the G9a and GLP

proteins was detected by western blot analysis at the indicated time point. α-tubulin was used as an internal control. (C) Immunoprecipitation-western blot to detect RA-induced Prdm12 proteins. P19 cells were cultured in bacterial grade dishes or cell culture dishes with or without 1 μM RA for 4 days. Cell lysates were subjected to immunoprecipitation followed by western blot analysis both with anti-Prdm12 antibody. IgG: Negative control for Immunoprecipitation. ★, Predicted size of Prdm12 (40 kDa).

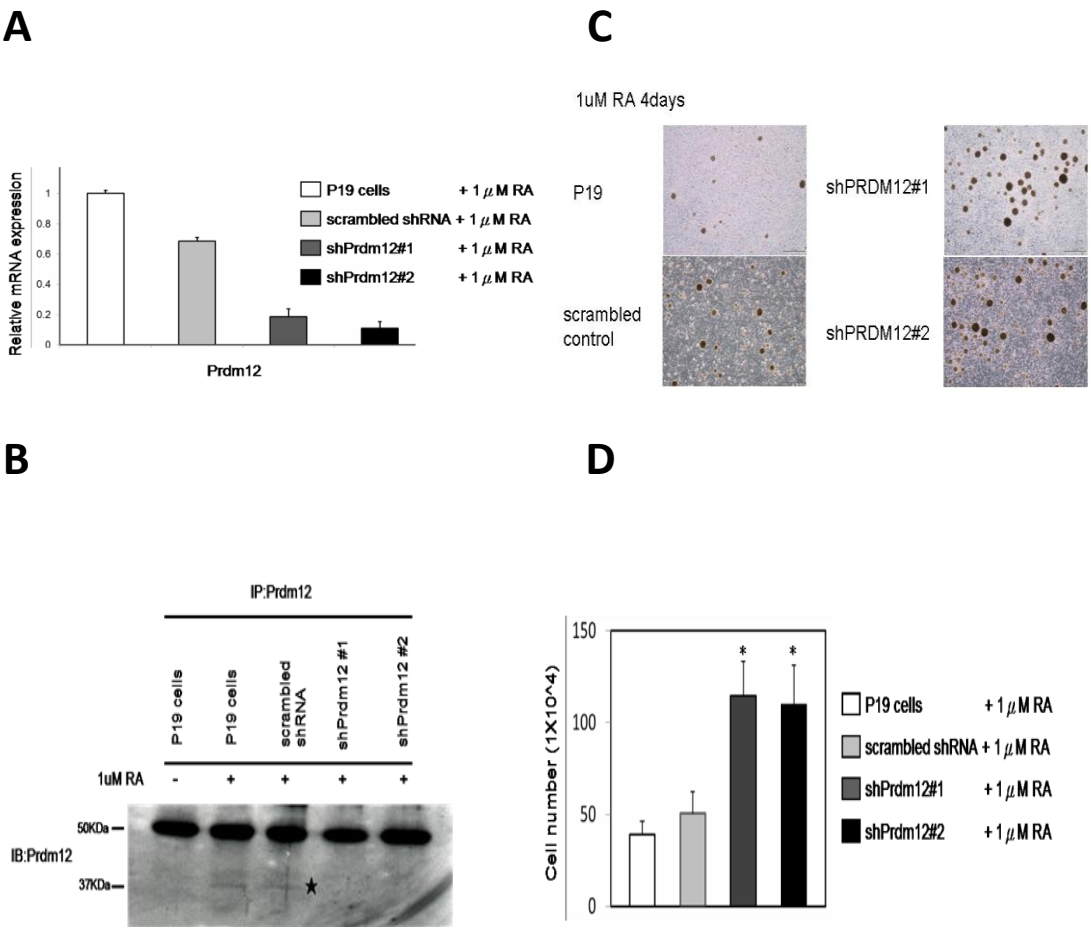

Fig.2-9: Prdm12 decreases cell proliferation in P19 cells. (A–B) Knockdown of Prdm12 in P19 cells. P19 cells were infected with indicated shRNA vectors. The stable Prdm12 knockdown cells incubated with 1 μM RA for 96 h in bacteria grade dishes. Quantitative RT-PCR (A) or western blotting (B) were performed to detect the knockdown efficiency of shPrdm12. ★, Predicted size of Prdm12 (40 kDa). (C-D) $1X10^6$ of indicated cells were seeded in bacteria grade dishes with 1 μM RA. After 96 h, cells were taken photo by Olympus IX 71 microscope, then trypsinized to count viable cells by Trypan Blue dye staining. Bars, SD. *$p < 0.05$ versus scrambled shRNA control.

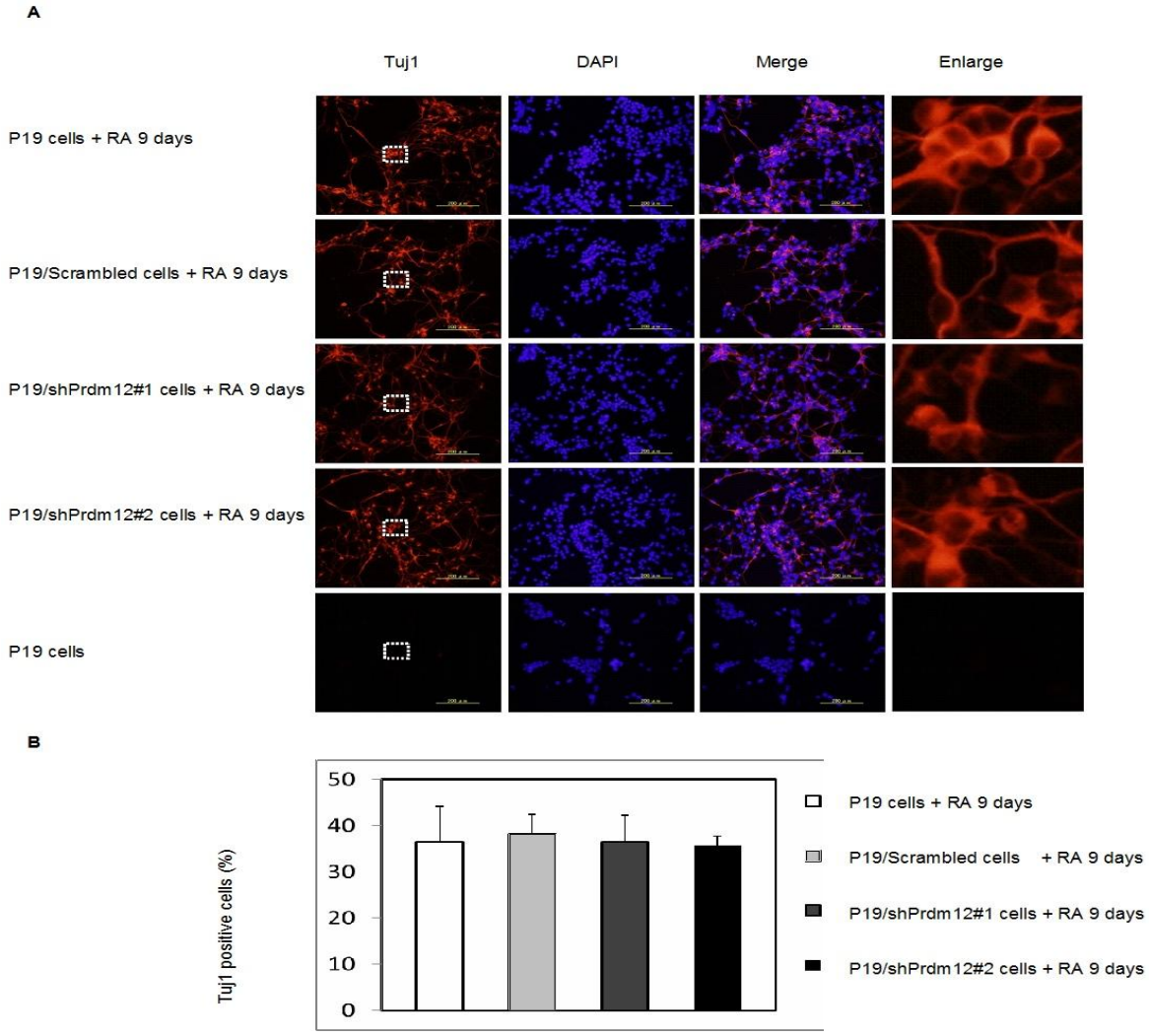

Fig. 2-10. Knockdown of Prdm12 does not affect the percentage of Tuj1-positive cells. P19 cells and P19/shPrdm12 cells were differentiated by RA as described in Materials and Methods. (A) Cells were fixed at day 9, then stained with anti-Tuj1 antibody, a marker for mature neurons. Tuj1-positive cells were labeled by goat anti-mouse IgG Alexa 568 secondary antibody (red). DAPI staining (blue) was used to visualize the cell nucleus. The region marked by the white box is shown at higher magnification in the right. Images were visualized by Olympus IX 71 microscopes. (B) Histograms showing the percentage of Tuj1-positive neurons at day 9. Error bars indicate_S.D.

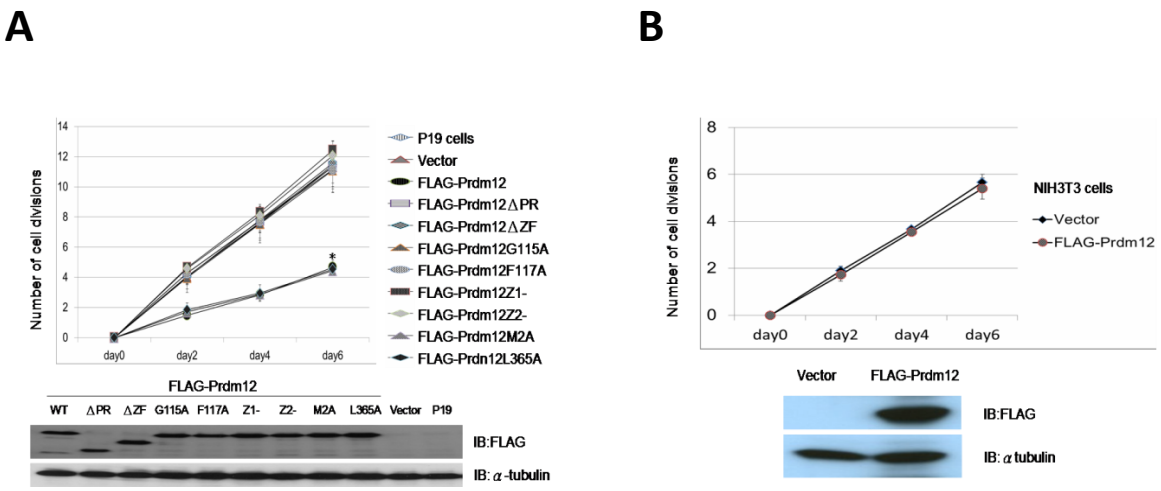

Fig. 2-11: (A) Growth curves of FLAG-Prdm12-overexpressing P19 cells. P19 cells were transfected with the indicated vectors. After selection, $1X10^5$ pool cells were seeded onto 6 well plates and counted every 48 h for 6 days. The growth curve was presented in cell division times (top). Bars, SD. *p < 0.05 versus control cells. Expression levels of FLAG-Prdm12 and mutants were detected by western blot with anti-FLAG antibodies for Prdm12 protein (bottom) and α-tubulin as the internal control. (B) Prdm12 does not affect cell proliferation in NIH-3T3 cells. NIH-3T3 cells were transfected with an empty construct or a construct expressing FLAG-Prdm12. After selection, cell growth curves of stable FLAG-Prdm12-expressing NIH-3T3 cells and control cells were determined as described in (A). Bars, SD. Expression of FLAG-Prdm12 was detected by western blot analysis with an anti-FLAG antibody.

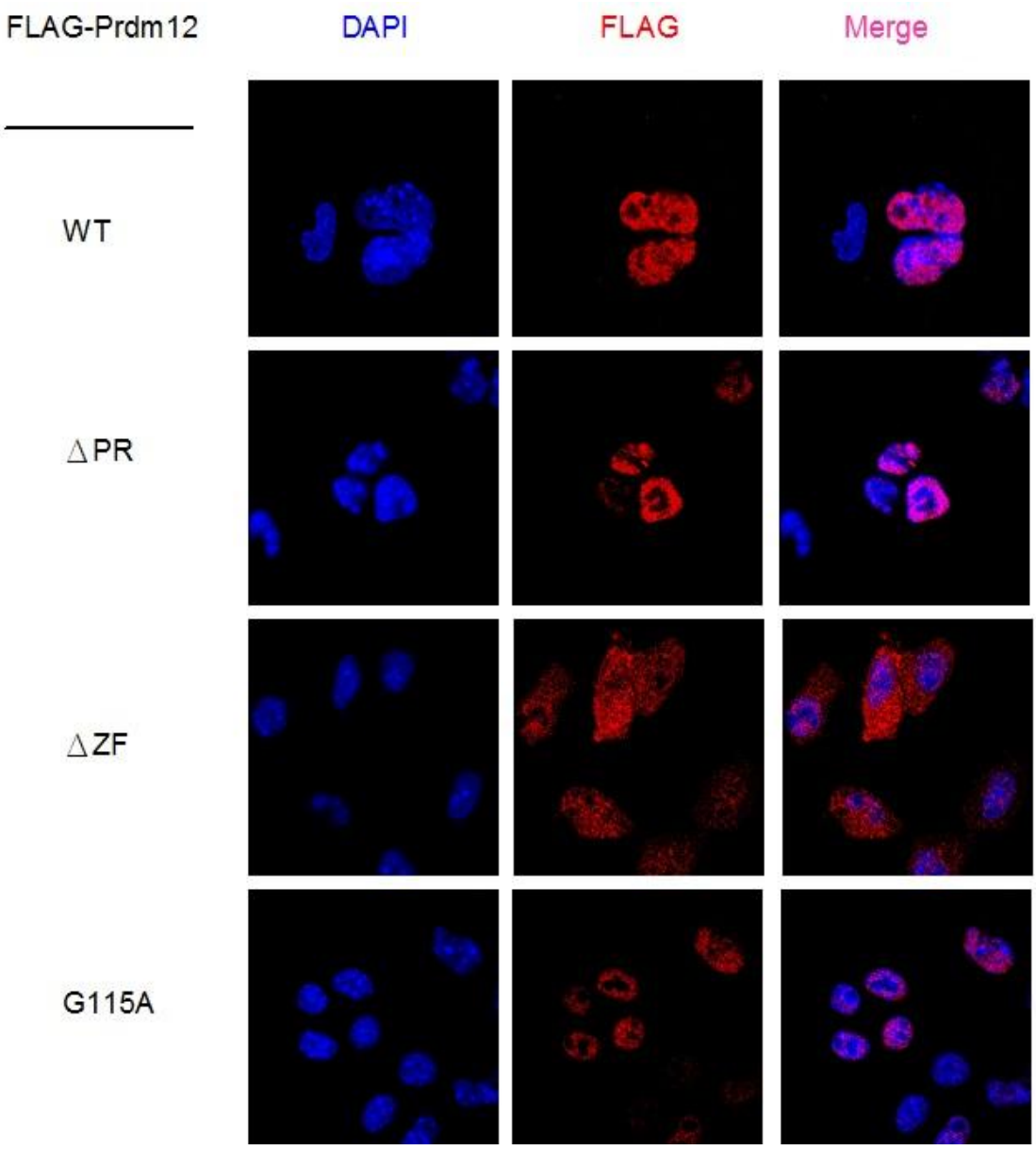
FLAG-Prdm12
DAPI
FLAG
Merge
WT
ΔPR
ΔZF
G115A

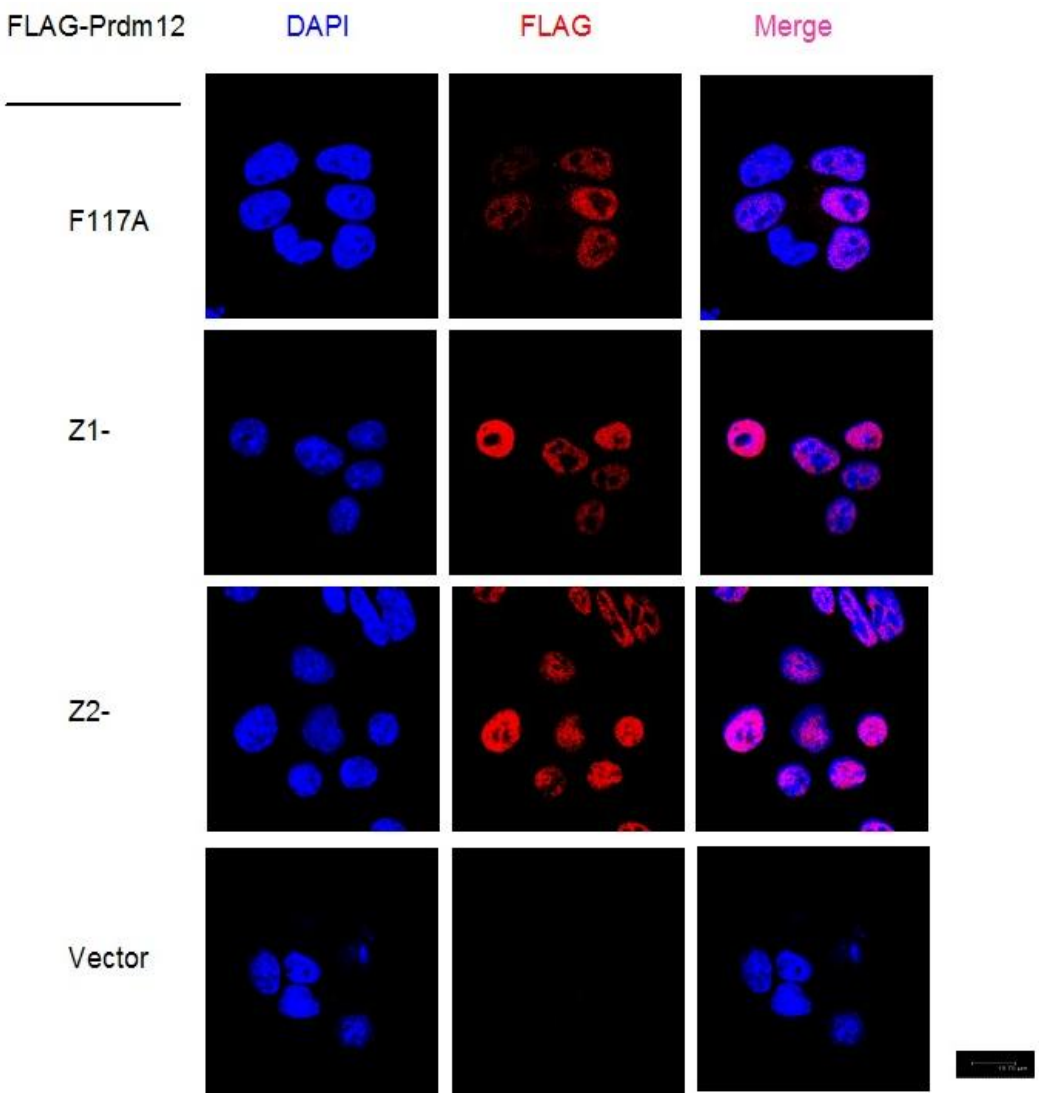

Fig. 2-12 : Plasmids expressing FLAG-Prdm12 or mutants were transfected into P19 cells. After fixation, cells were immunostained with anti-FLAG antibodies and labeled by goat anti-mouse IgG Alexa 568 secondary antibody for overexpressed proteins (red). DAPI staining (blue) for cell nucleus. Images were visualized by confocal microscopy.

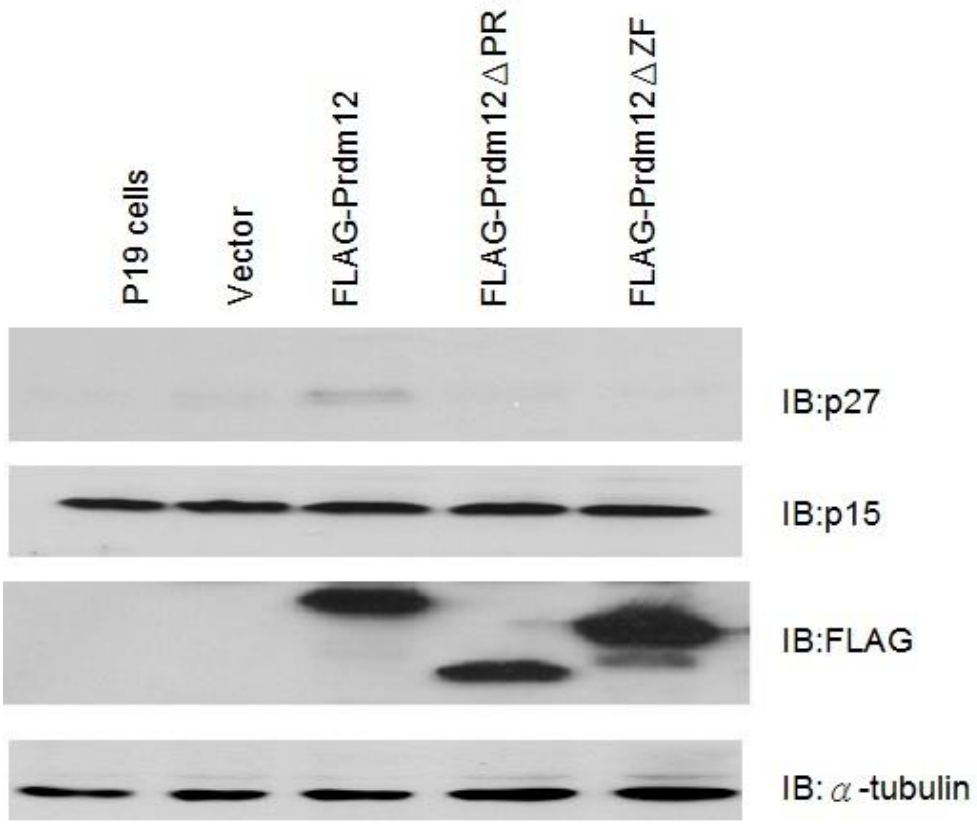

Fig. 2-13: Upregulation of p27 by overexpressing Prdm12 in P19 cells. When cells were harvested for the cell cycle analysis as described in Table I, a proportion of the cells were subjected to western blot analysis with anti-p15, anti-p27, and anti-FLAG antibodies for p15, p27, and the overexpressed Prdm12 proteins. α-tubulin was used as an internal control. The expression of p15 was not changed. p27 was increased in P19/FLAG-Prdm12 cells.

Table Ⅰ: Effect of Prdm12 on cell cycle of P19 cells.

	%G1(SD)	%S(SD)	%G2/M(SD)
P19 cells	20.67(3.66)	57.62(7.04)	19.93(3.83)
Vector	20.62(2.49)	57.77(4.66)	19.55(3.24)
FLAG-Prdm12	＊25.77(2.85)	56.08(3.41)	15.47(1.70)
FLAG-Prdm12ΔPR	20.33(1.81)	58.1(6.07)	20.07(5.15)
FLAG-Prdm12ΔZF	20.22(2.72)	58.9(5.80)	19.07(4.15)

$1X10^6$ cells expressing indicated proteins were plated to 10-cm cell culture dishes for 24 h. Cell cycle was measured by flow cytometry as described in Materials and Methods. ＊, $p<0.05$ versus control cells.

Chapter 3: Discussion

3-1 Potential role of Prdm12 in neurogenesis

Retinoic acid has been reported to increase the number of G_1-phase cells and the expression of p27 in P19 cells (Sasaki *et al.*, 2000; Pao *et al.*, 2011). In this paper, ectopic Prdm12 has been described to have the same function in P19 cells. In addition, it has been demonstrated that RA could induce the expression of Prdm12. Putative RARβ-response elements in the promoter region of Prdm12 have been predicted by transcription element search system analysis (data not shown). Furthermore, Prdm12 was found to be expressed in the dorsal root ganglia (DRG) of the mouse embryo (Kinameri *et al.*, 2008), and RARβ2 was upregulated by RA in embryonic DRG neurons (Corcoran *et al.*, 2000). Considering these findings, Prdm12 may play a role downstream of RARβ2 in the RA signaling pathway. This hypothesis could be examined using RARβ2 antagonists or analogues. This direction is worth pursuing because RA induces axon outgrowth in embryonic DRG neurons through activation of RARβ2, and because the RA signaling pathway is activated in injured neurons (Wong *et al.*, 2006). In

addition, Prdm14 is required for axon growth in primary motor neurons in zebrafish (Liu *et al.*, 2012). If Prdm12 is transcriptionally activated by RARβ2, it may have a role in axon regeneration.

Prdm14 maintains the human ES cell identity and represses the expression of differentiation marker genes (Tsuneyoshi *et al.*, 2008; Chia *et al.*, 2010). Prdm12 has antiproliferative effects on P19 cells but not on NIH3T3 cells (Fig. 2-11). This finding suggests that Prdm12 regulates a pathway specifically activated in “stem” cells.

3-2 HKMTase activity of Prdm12

This study has demonstrated, using an *in vitro* model, that Prdm12 interacts with G9a to mediate HKMTase activity (Fig. 2-5). Prdm1 also functions to recruit G9a through ZF domains, and G9a activity is required for Prdm1 to repress the transcription of target genes (Gyory *et al.*, 2004). Transcriptional regulation by Prdm12 involving G9a and/or G9a-mediated H3K9 dimethylation (a silencing mark) would indicate that Prdm12 targeted to the promoter region induces transcriptional repression. Therefore, this study suggests that Prdm12 indirectly increases the

expression of p27 by repressing the transcription of a negative regulator(s) of p27. It has been reported recently that retinal progenitor cells lacking G9a show defects in differentiation and proliferation, but photoreceptor precursors lacking G9a still develop into normal retina (Katoh *et al.*, 2012). This result indicates that G9a has a stage- or lineage-specific role(s) in proliferation and differentiation, and that it may be involved in the Prdm12-mediated function(s) of neuronal cells.

ZF domains are not only required for G9a interactions. Fig. 2-12 shows that the Prdm12 ZF domain contains nuclear localization signals (NLS) for its nuclear localization. Although the PR domain is not needed for H3K9 methylation, both the PR domain and ZF domains are necessary for Prdm12 to decrease cell proliferation in a gain-of-function model, and each domain alone is not sufficient for Prdm12's antiproliferative activity (Fig. 2-11). The PR and ZF domains have been reported to be required for Prdm4 to inhibit the cell cycle through transcriptional repression of cyclin E (Chittka *et al.*, 2004). Therefore, the properties of Prdm12 demonstrated in this study are similar to those of other Prdms.

3-3 Prmd12 as a potential tumor suppressor

Aside from their functions in differentiation, several Prdms act as tumor suppressors, and mutations or deletions frequently occur in these Prdm genes (Fog *et al.*, 2012). In activated B cell-like diffuse large cell lymphomas, Prdm1 deficiency increases tumor growth in mouse models (Mandelbaum *et al.*, 2010). Prdm5 is repressed in colorectal and gastric cancers (Watanabe *et al.*, 2007; Shu *et al.*, 2011). In contrast, overexpression of Prdm5 causes cell cycle arrest and apoptosis in cancer cells (Deng *et al.*, 2004). Deletion of DNA regions encoding Prdm12 has been reported in 15% of chronic myeloid leukemia (CML) patients (Reid *et al.*, 2004). Furthermore, Prdm2 is downregulated in CML (Lakshmikuttyamma *et al.*, 2009), and overexpression of Prdm2 in CML cell lines increases apoptosis and promotes cell differentiation (Pastural *et al.*, 2007). RA is currently used in differentiation therapy for acute promyelocytic leukemia (APL) patients (Kamimura *et al.*, 2011). In CML cell lines, RA cooperates with α-interferon (IFNα) to inhibit cell growth (Benthin *et al.*, 2001). These findings suggest that Prdm12 is a good candidate tumor suppressor in CML. Investigating whether Prdm12 is

involved in the RA signaling pathway may contribute to the understanding of RA mechanisms in CML.

3-4 Conclusion

In this study, Prdm12 was demonstrated to di-methylate H3K9 by recruiting G9a through ZF domain and exhibit antiproliferative effects in P19 cells. The findings of this study provide some insights into the role(s) of Prdm12 in neural development.

Chapter 4: Materials and methods

4-1 **Plasmids and cloning**

Full-length Prdm12 cDNA was amplified by PCR from an EST clone (image #6734548) purchased from the IMAGE consortium. For the generation of expression plasmids, amplified Prdm12 cDNA was inserted into pEGFP-C2 (Clontech, Mountair View, CA, USA), pGEX4T-1 (GE Healthcare, Little Chalfont, UK), or pCAG-FLAG-IRES-Puro vectors at specific restrict enzyme sites in frame with the indicated tag. To make Prdm12 deletion and point mutants, mutated fragments were created by PCR amplification and were subcloned into a pCAG-FLAG-IRES-Puro vector. Glutathione S-transferase (GST)-tagged H3N, mutants, and GST-G9aSET have been described earlier (Tachibana *et al*. 2001). Three oligonucleotides of short hairpin RNAs (shRNA) targeting the Prdm12 gene were designed and synthesized from Sigma (St. Louis, MO, USA) then inserted into a pSUPER.retro.puro vector (OligoEngine, Seattle, WA).

4-2 **Cell culture and differentiation**

HEK293T, NIH3T3, and P19 cells were cultured in Dulbecco's Modified

Eagle Medium (DMEM, Nissui Pharmaceutical Co. Ltd.) supplemented with 10% fetal bovine serum (FBS), 100 μg/ml streptomycin, and 100 U/ml penicillin (Gibco, Carlsbad, CA, USA) at 37°C in a 5% CO2 atmosphere. To induce neural differentiation, 1×10^6 P19 cells were cultured on 10 cm bacteria grade dishes for aggregation in DMEM supplemented with 10% FBS and 1 μM RA (solved in 99.9% EtOH; Sigma). After 96 h, cells were trypsinized then transferred to poly-L-lysine (Sigma) coated tissue culture dishes at a density of 1×10^5 cells/ml in 10% FBS DMEM without RA. After 24 h, the medium was changed to 0.5% FBS DMEM to induce neural differentiation for another 96 h. All media were replaced with fresh media every 48 h.

4-3 **Transfection and infection of cells**

HEK293T, NIH3T3, and P19 cells were seeded in 6-well culture plate for 24 h before transfection. Two micrograms of indicated plasmids were transfected into HEK293T cells using TransIT-LT-1 reagent (Mirus Bio corp., Madison, WI, USA) or 4 μg of plasmids were transfected into NIH3T3 and P19 cells using Lipofectamine 2000 reagent (Invitrogen, Carlsbad, CA, USA)

according to the manufacturer's instructions. For infection, GP2-293 cells were co-transfected with a pSUPER.retro.puro vector containing the shRNA against mouse Prdm12 and a pVSV-G vector. After 48 h, the culture media was filtered with a 0.45-µm filter then used to infect P19 cells with polybrene (8 µg/ml). To establish stable cell lines, cells were treated with 1 µg/ml puromycin for five days.

4-4 ***In Vitro*** **Histone methyltransferase (HMTase) assay**

HMTase assays was performed as described (Tachibana *et al*. 2001), with some modifications. Briefly, 10 µl of reaction mixture containing 2 µg of core histones, immunoprecipitated enzymes, and 125 nCi of S-adenosyl-[methyl-14C]-L-methionine in assay buffer (50 mM Tris, pH 8.5, 5 mM DTT) were incubated for 1 h at 30°C. Proteins were separated by 15% SDS–PAGE and visualized by coomassie brilliant blue staining. Detection of methyl-14C was performed by using a BAS-5000 imaging analyzer (Fuji Film).

4-5 **Immunoprecipitation and immunocytochemistry**

After 48 h of transfection (or at the harvesting times indicated), cells were lysed in lysis buffer containing 20 mM Hepes, pH 7.5, 420 mM NaCl, 1.5 mM MgCl2, 0.1% NP-40, and protease inhibitor cocktail (Nacalai Tesque, Kyoto, Japan). Supernatants were collected by centrifugation then incubated with 0.5–1 μg antibody overnight at 4°C and subsequently isolated by protein G-agarose (GE Healthcare). Immunoprecipitants were washed extensively with lysis buffer then used in Western blot or in vitro HMTase assays. For immunocytochemistry, cells were washed with PBS and fixed in 4% paraformaldehyde at room temperature for 10 min. After two washes with PBS, cells were permeabilized and blocked with 0.1% Triton X-100/5% BSA/PBS at room temperature for 30 min. First antibodies were added as follow: anti-FLAG (1:1000, Sigma), anti-Prdm12 (1:500, made by our Lab) in 1% BSA/PBS at 37℃ for 1 h. After three washes with 1% Tween/PBS, anti-mouse IgG Alexa 568 or anti-rabbit IgG Alexa 488 (1:1000, Invitrogen) with DAPI (1:3000, Sigma) were added at room temperature for 1 h. After three washes with 1% Tween/PBS then mounted in Vectashield (Vector). Slides were analyzed using a TSC SP3

(Leica) confocal microscope.

4-6 **Antibodies**

The commercially available primary antibodies used were as follows: mouse monoclonal antibodies to FLAG M2 (F3165; Sigma); GFP (11 814 460 001; Roche, Mannheim, Germany); G9a (A8620A, Perseus Proteomics Inc., Tokyo, Japan); p27 (K25020; BD Biosciences, San Jose, CA); G9a (A8620A, Perseus Proteomics Inc., Tokyo, Japan); GLP (#422, Perseus Proteomics Inc.); Neuronal Class III β-Tubulin (Tuj1, MMS-435P; Covance, Princeton, USA); p27 (K25020; BD Biosciences, San Jose, CA); α-tubulin (T-5168, Sigma) and normal rabbit IgG (sc-2027; Santa Cruz Biotechnology, Santa Cruz, CA); and rabbit polyclonal antibodies to p15 (#4822; Cell Signaling, Danvers, MA). Secondary antibodies were as follows: peroxidase-conjugated mouse or rabbit IgG secondary antibodies (NA931V and NA934V; GE Healthcare) and anti-mouse IgG Alexa 568 and anti-rabbit IgG Alexa 488 (A11004 and A11008; Invitrogen). The antibodies generated from our laboratory were as follows: rabbit polyclonal antibodies to Prdm4, Prdm6, Prdm12 and Prdm13.

4-7 **Anti-Prdm12 antibody generation**

To generate rabbit anti-Prdm12 polyclonal antibodies, cDNA fragments corresponding to residues N43–F230 of mouse Prdm12 were subcloned into pGEX-4T-1, then the fusion protein (GST-Prdm12 (43-230)) was purified and immunized into a rabbit (Hokudo Co., Ltd., Sapporo, Japan).

BL21 competent cells transformed with pGEX4T-1-Prdm12 (43-230) or pGEX4T-1 were cultured at 4 ml LB overnight then transferred to 500 ml LB. Cells were incubated until OD600 reached 0.5 and IIsopropyl-1-thio-β-Dgalactopyranoside (IPTG) was added to a final concentration of 200 μM. After 3 h, cell pellets were collected and stored at -80°C at least 1 h, then resuspended in 20 ml RIPA buffer (140mM NaCl, 10mM Tris, pH 8, 1mM EDTA, 1% Triton X-100, 0.1% SDS, 0.1% deoxycholic acid). After sonication, supernatant was collected by centrifugation at 10000 g for 10 minutes. 2 ml glutathione sepharose beads were added to supernatant. After 4°C rotation overnight, beads were washed by 5 ml RIPA buffer 3 times, then 1.5 ml 20mM dimethyl pimelimidate (DMP) in 200 mM HEPES crosslinking buffer was added for cross-link. After 1 h rotation at room temperature, 1.5 ml 200mM ethanolamine was added and beads were

incubated for 30 minutes at room temperature with rotation. Then beads were washed as follows: TBS (25 mM Tris-Cl, pH 7.5, 150 mM NaCl) 2 times, elution buffer (150 mM NaCl, 200 mM Glycine-HCl, pH 2.0) 5 time, and TBS 2 times. First 2 ml serum was mixed with GST-beads then rotated for 30 minutes at 4°C. Next, serum was transferred to column with GST-Prdm12 (43-230)-beads. After incubation, column was washed by 1 ml TBS 3 times, 2 ml wash buffer (500 mM NaCl, 20 mM Tris, pH 7.5, 0.1% Triton X-100) 2 times and 1 ml TBS again 2 times, then 250 µl elution buffer was added to elute antibodies. 10 fractions were collected in tube with 32 µl 2M Tris (pH 8.8). Fractions contained antibodies were combined and dialyzed in PBS buffer.

4-8 **Cell counting and cell cycle analysis**

FLAG-Prdm12 or mutants overexpressing P19 cells were seeded in 6 well plates at a density of 1×10^5 cells/well. Cell numbers were counted under a light microscope by trypan blue exclusion every 48 h for 6 days. The division times were calculated according to the following formula: (lgND−lgN0)/ lg2, where N0 is the cell number on the day of seeding, and

ND is the cell number after culture for 2, 4, or 6 days. For cell cycle analysis, 1×10^6 FLAG-Prdm12 or mutants overexpressing P19 cells were seeded into 10-cm culture dishes. After 24 h, cells were collected and washed in PBS before fixing in cold 75% ethanol for 1 h at -20°C. After three washes with cold PBS, fixed cells were incubated with 50 mg/ml propidium iodide, 10 mg/ml RNase A, and 0.1% Triton X-100 at least 30 min before analysis. The cell cycle was analyzed using a BD FACS Calibur flow cytometer (BD Biosciences,), and the cell cycle analysis was done by Dean-Jett-Fox method of FlowJo software.

4-9 **Quantitative RT-PCR**

Total RNAs were isolated with Sepasol-RNA I (Nacalai Tesque) on the indicated days after RA treatment and cDNA was synthesized using the Omniscript RT kit (QIAGEN, KJ Venlo, Netherlands) according to the manufacturer's instructions. Quantitative RT-PCR was performed with Power SYBR Green PCR Master Mix (Applied Biosystems, Warrington, UK) on a StepOne Plus Real-Time PCR System (Applied Biosystems). The primers used were Prdm12 forward 5´-CCCTTTTGGGGCTTCAGTTTC-3',

and reverse 5′-GGTCGCTCATTCTCTTGTTTGG-3′; G9a forward 5´-CACAAGCACATCGATGTGATT-3´, and reverse 5´-ATGGTAGTTGACAGCATGGAG-3´; Oct3⁄4 forward 5´-GAAGCAGAAGAGGATCACCTTG-3´, and reverse 5´-TTCTTAAGGCTGAGCTGCAAG-3´; Tuj1 forward 5´-TGGACAGTGTTCGGTCTGG-3´, and reverse 5´-CCTCCGTATAGTGCCCTTTGG-3´; GAPDH forward 5′-CATCTTCTTGTGCAGTGCCA-3′, and reverse 5′-CGTTGATGGCAACAATCTCC-3′. Gene expression was analyzed by the ΔΔ-CT method through StepOne Software 2.1 (Applied Biosystems).

4-10 **Primers**

List of Primers used for plasmid construction. F, forward primer; R, reverse primer.

FLAG-PRDM12-F: 5´-AAGCGGCCGCTATGATGGGCTCTGTGCTC-3´;

FLAG-PRDM12-R: 5´-TTAGATCTTCACAGCACCATGGCCGG-3´;

GFP-Prdm12-F: 5´-CGGAATTCATGATGGGCTCTGTGCTCCC-3´;

GFP-PRDM12-R: 5´- TTGGATCCTCACAGCACCATGGCCGG-3´;

GSTPrdm12Primer-F: 5´-CCGAATTCATGATGGGCTCTGTGCTCCC-3´

GSTPrdm12Primer-R: 5´-ATGCGGCCGCTCACAGCACCATGGCCGG-3´

PRDM12ΔSET-F: 5´-CTATCTAGCCTGGTGAATTCCCACAACACC-3´

PRDM12ΔSET-R: 5´-GGTGTTGTGGGAATTCACCAGGCTAGATAG-3´

PRDM12ΔZF-F: 5´-GACTCCGCGACCGGCGAGCGTCCCTACAAGTGC-3´

PRDM12ΔZF-R: 5´-GCACTTGTAGGGACGCTCGCCGGTCGCGGAGTC-3´

PRDM12-G115A-F: 5´-GAGATGGCTCCCTTCACTGGC-3´;

PRDM12-G115A-R: 5´-GCCAGTGAAGGGAGCCATCTC-3´;

PRDM12- F117A-F: 5´-TGGGCCCCGCTACTGGCCG-3´;

PRDM12- F117A-R: 5´-CGGCCAGTAGCGGGGCCCA-3´;

PRDM12Z1--F: 5´-ATGCGCCGAGTCATCCGACACCGC-3´;

PRDM12Z1--R: 5´-GCGGTGTCGGATGACTCGGCGCAT-3´;

PRDM12Z2--F: 5´-TTCGTGCGCCGCTTCCGCAACCGC-3´;

PRDM12Z2--R: 5´-GCGGTTGCGGAAGCGGCGCACGAA-3´;

FLAG-PRDM12M2A-F: 5´-AAGAATTCAATGGCTGGCTCTGTGCTCCC-3´;

FLAG-PRDM12L365A-R: 5´-TTAGATCTTCAAGCCACCATGGCCGG-3´;

shPRDM12#1-F:

5´-AGCTTAAAAAAGGTACAGTACGCTACTTCATCGTGACAGGAAGCGAT

GAAGTAGCGTACTGTACCGG-3´;

shPRDM12#1-R:

5´-GATCCCGGTACAGTACGCTACTTCATCGCTTCCTGTCACGATGAAGTAG

CGTACTGTACCTTTTTTA-3´;

shPRDM12#2-F:

5´-AGCTTAAAAAACTATAGAACGCAGTAATTAGAGTGACAGGAAGCTCTAAT

TACTGCGTTCTATAGGG-3´;

shPRDM12#2-R:

5´-GATCCCCTATAGAACGCAGTAATTAGAGCTTCCTGTCACTCTAATTACTGC

GTTCTATAGTTTTTTA-3´;

Scrambled shRNA-F:

5´-AGCTTAAAAAAGCCCGTGTTCATATCAAGACTGTGACAGGAAGCAGTCTTG

ATATGAACACGGGCGG-5´;

Scrambled shRNA-R:

5´-GATCCCGCCCGTGTTCATATCAAGACTGCTTCCTGTCACAGTCTTGATAT

GAACACGGGCTTTTTTA-5´.

Acknowledgements

I would like to express my gratitude to all those who helped me during the 6 years in Japan. A special acknowledgement should be shown to Professor Shinkai and Professor Tachibana, who gave me kind encouragement and useful instructions all through the process of pursuing my studies. Mikiko Fukuda, Tae Komai and all the members gave me supports not only for experimental techniques but also daily life. I am honored to be one of this vigorous laboratory. Finally, I want to thanks my parents and my wife for their love and support.

Even though I walk through the valley of the shadow of death, I will fear no evil, for you are with me; your rod and your staff, they comfort me.

- Psalm 23.4

Reference

Benthin, M., Dallmann, I., and Atzpodien, J. 2001. 13cis- and all-trans retinoic acid have antiproliferative effects on CML cells and render IFN alpha antiproliferative potency after combined treatment in vitro. Cancer biotherapy & radiopharmaceuticals 16, 323-331.

Chia, N.Y., Chan, Y.S., Feng, B., Lu, X., Orlov, Y.L., Moreau, D., Kumar, P., Yang, L., Jiang, J., Lau, M.S., et al. 2010. A genome-wide RNAi screen reveals determinants of human embryonic stem cell identity. Nature 468, 316-320.

Chittka, A., Arevalo, J.C., Rodriguez-Guzman, M., Perez, P., Chao, M.V., and Sendtner, M. 2004. The p75NTR-interacting protein SC1 inhibits cell cycle progression by transcriptional repression of cyclin E. The Journal of cell biology 164, 985-996.

Corcoran, J., Shroot, B., Pizzey, J., and Maden, M. 2000. The role of retinoic acid receptors in neurite outgrowth from different populations of embryonic mouse dorsal root ganglia. Journal of cell science 113 (Pt 14), 2567-2574.

Deng, Q., and Huang, S. 2004. PRDM5 is silenced in human cancers and has growth suppressive activities. Oncogene 23, 4903-4910.

Dillon SC, Zhang X, Trievel RC, Cheng X. 2005. The SET-domain protein superfamily: protein lysine methyltransferases. Genome Biol.;6(8):227. 2005 Aug 2. Review.

Fog, C.K., Galli, G.G., and Lund, A.H. 2012. PRDM proteins: important players in differentiation and disease. BioEssays : news and reviews in molecular, cellular and developmental biology 34, 50-60.

Gill, R.M., Slack, R., Kiess, M., and Hamel, P.A. 1998. Regulation of expression and activity of distinct pRB, E2F, D-type cyclin, and CKI family members during terminal differentiation of P19 cells. Experimental cell research 244, 157-170.

Gyory, I., Wu, J., Fejer, G., Seto, E., and Wright, K.L. 2004. PRDI-BF1 recruits the histone H3 methyltransferase G9a in transcriptional silencing. Nature immunology 5, 299-308.

Hernandez-Lagunas, L., Choi, I.F., Kaji, T., Simpson, P., Hershey, C., Zhou, Y., Zon, L., Mercola, M., and Artinger, K.B. 2005. Zebrafish narrowminded disrupts the transcription factor prdm1 and is required for neural crest and sensory neuron specification. Developmental biology 278, 347-357.

Hohenauer, T., and Moore, A.W. 2012. The Prdm family: expanding roles in stem cells and development. Development 139, 2267-2282.

Jones-Villeneuve, E.M., McBurney, M.W., Rogers, K.A., and Kalnins, V.I. 1982. Retinoic acid induces embryonal carcinoma cells to differentiate into neurons and glial cells. The Journal of cell biology 94, 253-262.

Kamimura, T., Miyamoto, T., Harada, M., and Akashi, K. 2011. Advances in therapies for acute promyelocytic leukemia. Cancer science 102, 1929-1937.

Katoh K, Yamazaki R, Onishi A, Sanuki R, Furukawa T. 2012. G9a histone methyltransferase activity in retinal progenitors is essential for proper differentiation and survival of mouse retinal cells. J Neurosci.5;32(49):17658-70

Kinameri, E., Inoue, T., Aruga, J., Imayoshi, I., Kageyama, R., Shimogori, T., and Moore, A.W. 2008. Prdm proto-oncogene transcription factor family expression and interaction with the Notch-Hes pathway in mouse neurogenesis. PloS one 3, e3859.

Komai, T., Iwanari, H., Mochizuki, Y., Hamakubo, T., and Shinkai, Y. 2009. Expression of the mouse PR domain protein Prdm8 in the developing central nervous system. Gene expression patterns : GEP 9, 503-514.

Kranenburg, O., Scharnhorst, V., Van der Eb, A.J., and Zantema, A. 1995. Inhibition of cyclin-dependent kinase activity triggers neuronal differentiation of mouse neuroblastoma cells. The Journal of cell biology 131, 227-234.

Lakshmikuttyamma, A., Takahashi, N., Pastural, E., Torlakovic, E., Amin, H.M., Garcia-Manero, G., Voralia, M., Czader, M., DeCoteau, J.F., and Geyer, C.R. 2009. RIZ1 is potential CML tumor suppressor that is down-regulated during disease progression. Journal of hematology & oncology 2, 28.

Liu, C., Ma, W., Su, W., and Zhang, J. 2012. Prdm14 acts upstream of islet2 transcription to regulate axon growth of primary motoneurons in zebrafish. Development 139, 4591-4600.

Maden, M. 2007. Retinoic acid in the development, regeneration and maintenance of the nervous system. Nature reviews Neuroscience 8, 755-765.

Mandelbaum, J., Bhagat, G., Tang, H., Mo, T., Brahmachary, M., Shen, Q., Chadburn, A., Rajewsky, K., Tarakhovsky, A., Pasqualucci, L., et al. 2010. BLIMP1 is a tumor suppressor gene frequently disrupted in activated B cell-like diffuse large B cell lymphoma. Cancer cell 18, 568-579.

Pao, P.C., Huang, N.K., Liu, Y.W., Yeh, S.H., Lin, S.T., Hsieh, C.P., Huang, A.M., Huang, H.S., Tseng, J.T., Chang, W.C., et al. 2011. A novel RING finger protein, Znf179, modulates cell cycle exit and neuronal differentiation of P19 embryonal carcinoma cells. Cell death and differentiation 18, 1791-1804.

Pastural, E., Takahashi, N., Dong, W.F., Bainbridge, M., Hull, A., Pearson, D., Huang, S., Lowsky, R., DeCoteau, J.F., and Geyer, C.R. 2007. RIZ1 repression is associated with insulin-like growth factor-1 signaling activation in chronic myeloid leukemia cell lines. Oncogene 26, 1586-1594.

Reid, A.G., and Nacheva, E.P. 2004. A potential role for PRDM12 in the pathogenesis of chronic myeloid leukaemia with derivative chromosome 9 deletion. Leukemia 18,

178-180.

Ross, S.E., McCord, A.E., Jung, C., Atan, D., Mok, S.I., Hemberg, M., Kim, T.K., Salogiannis, J., Hu, L., Cohen, S., et al. 2012. Bhlhb5 and Prdm8 form a repressor complex involved in neuronal circuit assembly. Neuron 73, 292-303.

Sasaki, K., Tamura, S., Tachibana, H., Sugita, M., Gao, Y., Furuyama, J., Kakishita, E., Sakai, T., Tamaoki, T., and Hashimoto-Tamaoki, T. 2000. Expression and role of p27(kip1) in neuronal differentiation of embryonal carcinoma cells. Brain research Molecular brain research 77, 209-221.

Shu, X.S., Geng, H., Li, L., Ying, J., Ma, C., Wang, Y., Poon, F.F., Wang, X., Ying, Y., Yeo, W., et al. 2011. The epigenetic modifier PRDM5 functions as a tumor suppressor through modulating WNT/beta-catenin signaling and is frequently silenced in multiple tumors. PloS one 6, e27346.

Sun, X.J., Xu, P.F., Zhou, T., Hu, M., Fu, C.T., Zhang, Y., Jin, Y., Chen, Y., Chen, S.J., Huang, Q.H., et al. 2008. Genome-wide survey and developmental expression mapping of zebrafish SET domain-containing genes. PloS one 3, e1499.

Tachibana, M., Sugimoto, K., Fukushima, T., and Shinkai, Y. 2001. Set domain-containing protein, G9a, is a novel lysine-preferring mammalian histone methyltransferase with hyperactivity and specific selectivity to lysines 9 and 27 of histone H3. The Journal of biological chemistry 276, 25309-25317.

Tachibana, M., Sugimoto, K., Nozaki, M., Ueda, J., Ohta, T., Ohki, M., Fukuda, M., Takeda, N., Niida, H., Kato, H., et al. 2002. G9a histone methyltransferase plays a dominant role in euchromatic histone H3 lysine 9 methylation and is essential for early embryogenesis. Genes & development 16, 1779-1791.

Tsuneyoshi, N., Sumi, T., Onda, H., Nojima, H., Nakatsuji, N., and Suemori, H. 2008. PRDM14 suppresses expression of differentiation marker genes in human embryonic stem cells. Biochemical and biophysical research communications 367, 899-905.

Volkel, P., and Angrand, P.O. 2007. The control of histone lysine methylation in epigenetic regulation. Biochimie 89, 1-20.

Wang, Y., Sun, Y., and Qiao, S. 2012. ADAM23 knockdown promotes neuronal differentiation of P19 embryonal carcinoma cells by up-regulating P27KIP1 expression. Cell biology international 36, 1275-1279.

Watanabe, Y., Toyota, M., Kondo, Y., Suzuki, H., Imai, T., Ohe-Toyota, M., Maruyama, R., Nojima, M., Sasaki, Y., Sekido, Y., et al. 2007. PRDM5 identified as a target of epigenetic silencing in colorectal and gastric cancer. Clinical cancer research : an official journal of the American Association for Cancer Research 13, 4786-4794.

Wong, L.F., Yip, P.K., Battaglia, A., Grist, J., Corcoran, J., Maden, M., Azzouz, M., Kingsman, S.M., Kingsman, A.J., Mazarakis, N.D., et al. 2006. Retinoic acid receptor

beta2 promotes functional regeneration of sensory axons in the spinal cord. Nature neuroscience 9, 243-250.

Zhang, H., and Rosdahl, I. 2004. Expression of p27 and MAPK proteins involved in all-trans retinoic acid-induced apoptosis and cell cycle arrest in matched primary and metastatic melanoma cells. International journal of oncology 25, 1241-1248.